12-2015

Robust Modeling Framework for Transportation Infrastructure System Protection Under Uncertainty

Jie Lu
Clemson University

ROBUST MODELING FRAMEWORK FOR TRANSPORTATION INFRASTRUCTURE SYSTEM PROTECTION UNDER UNCERTAINTY

A Dissertation
Presented to
The Graduate School of
Clemson University

In Partial Fulfillment
of the Requirements for the Degree
Doctor of Philosophy
Civil Engineering

---

by
Jie Lu
December 2015

Accepted by:
Dr. Yongxi Huang, Committee Chair
Dr. Sez Atamturktur, Co-Chair
Dr. Akshay Gupte,
Dr. C. Hsein Juang

Abstract

This dissertation presents a modelling framework that will be useful for decision makers at federal and state levels to establish efficient resource allocation schemes to transportation infrastructures on both strategic and tactical levels. In particular, at the upper level, the highway road network carries traffic flows that rely on the performance of individual bridge infrastructure which is optimized through robust design at lower level. A system optimization model is developed to allocate resources to infrastructure systems considering traffic impact, which aims to reduce infrastructure rehabilitation cost, long term economic cost including travel delays due to realization of future natural disasters such as earthquakes. At the lower level, robust design for each individual bridge is confined by the resources allocated from upper level network optimization model, where optimal rehabilitation strategies are selected to improve its resiliency to hedge against potential disasters. The above two decision making processes are interdependent, thus should not be treated separately. Thus, the resultant modeling framework will be a step forward in the disaster management for transportation infrastructure network.

This dissertation first presents a novel formulation and a solution algorithm of network level resource allocation problem. A mean-risk two-stage stochastic programming model is developed with the first-stage considering resources allocation and second-stages shows the response from system travel delays, where the conditional value-at-risk (*CVaR*) is specified as the risk measure. A decomposition method based on generalized Benders decomposition is developed to solve the model, with a concerted effort on overcoming

the algorithmic challenges imbedded in non-convexity, nonlinearity and non-separability of first- and second- stage variables.

The network level model focusing on traffic optimization is further integrated into a bi-level modeling framework. For lower level, a method using finite element analysis to generate a nonlinear relationship between structural performances of bridges and retrofit levels. This relationship was converted to traffic capacity-cost relationship and used as an input for the upper-level model. Results from the Sioux Falls transportation network demonstrated that the integration of both network and FE modeling for individual structure enhanced the effectiveness of retrofit strategies, compared to linear traffic capacity-cost estimation and conventional engineering practice which prioritizes bridges according to the severity of expected damages of bridges.

This dissertation also presents a minimax regret formulation of network protection problem that is integrated with earthquake simulations. The lower level model incorporates a seismic analysis component into the framework such that bridge columns are subject to a set of ground motions. Results of seismic response of bridge structures are used to develop a Pareto front of cost-safety-robustness relationship from which bridge damage scenarios are generated as an input of the network level model.

Acknowledgement

First of all, I would like to express my deepest gratitude to my advisors, Professor Yongxi Huang and Professor Sez Atamturktur for their excellent tutoring, advice and remarkable patience. I thank you for your enlightening ideas and extensive knowledge about transportation engineering, operations research and structural assessment.

I would also like to show my great appreciation to other committee members, Professor Akshay Gupte and Professor C. Hsein Juang, for spending their time and efforts in providing guidance, comments and suggestions to improve my Ph.D. dissertation. My thanks also go to the entire transportation faculty from whom I learned the knowledge of transportation engineering.

Additionally, I would like to thank my friends and colleagues Fei Xie, Shengyin Li, Chaofeng Wang, Saurabh Prabhu, Wenping Gong, and Marcos Martínez; their comments and support have been valuable. I would also thank a number of other friends, including Chongze Hu, Fanfu Fan, Xiaoyu Hu and Bin Pei, for making my life at Clemson so enjoyable.

Finally, I would like to thank my parents who supported my pursuit of doctoral education. I also thank my wife, Suwan Shen, for her endless love and support during the entire doctoral program, and always standing by my side. This dissertation is dedicated to them all.

Table of Contents

Table of Contents (Continued)

Chapter Page

Table of Contents (Continued)

List of Figures

List of Figures (Continued)

Figure Page

List of Tables

Chapter 1 Introduction

1 Background and motivation

Transportation infrastructure systems, such as road networks and highway bridges, play an essential role in the economy and sustain the economic growth of the United States. From 1980 to 2010, the U.S. total number of motor vehicles has increased 92% and vehicle-miles of travels has increased 53% while the total highway lane-miles has only increased merely 10% (Federal Highway Administration, 2010, 2013).The situation is exacerbating due to the limited funding for maintenance. Delayed maintenance has resulted in even more degradation to the aging and deteriorating transportation networks.

In a transportation infrastructure system, bridge structures are crucial components that should assure life safety and transport efficiency. However, bridges are extremely vulnerable to natural hazards compared to other components in the transportation system, such as highway roads. Thus, they are often considered to be the weakest links in a network. Physical damages and traffic carrying capacity losses to the bridges in a transportation system not only affect short term evacuation and emergency response, but also influence long term residential and commercial activities.

The modelling framework proposed in this dissertation will be useful for decision makers at federal and state levels to establish efficient resource allocation schemes to transportation infrastructures on both strategic and tactical levels. In particular, at the

upper level, the highway road network carries traffic flows that rely on the performance of individual bridge infrastructure which is optimized through robust design at lower level. A system optimization model is developed to allocate resources to infrastructure systems considering traffic impact, which aims to reduce infrastructure rehabilitation cost, long term economic cost including travel delays due to realization of future natural disasters such as earthquakes. At the lower level, robust design for each individual bridge is confined by the resources allocated from upper level network optimization model, where optimal rehabilitation strategies are selected to improve its resiliency to hedge against potential disasters.

The above two decision making processes are interdependent, thus should not be treated separately. Thus, the resultant modeling framework will be a step forward in the disaster management for transportation infrastructure network. The proposed bi-level modeling framework is novel because it integrates both ideas of top-down and bottom-up resources allocation strategies by considering interaction of structure rehabilitation and transportation system performance. Research efforts from multiple disciplines are integrated in this framework including transportation network modeling, engineering economics, and structural engineering.

2 Objectives

The main objectives of this dissertation are to: (1) improve the fundamental understanding of the infrastructure rehabilitation scheme that integrates the effects of

networked infrastructures and the structural functionality improvement under budget limits; (2) create a novel, interactive bi-level resource allocation modeling framework to improve, by the most efficient means, the infrastructure resilience and social welfares.

3. Organization of the dissertation

This dissertation is organized into chapters described below.

Chapter 2 describes a novel formulation and a solution algorithm of network level problem. A mean-risk two-stage stochastic programming model is developed with the first-stage considering resources allocation and second-stages shows the response from system travel delays, where the conditional value-at-risk (*CVaR*) is specified as the risk measure. A decomposition method based on generalized Benders decomposition is developed to solve the model, with a concerted effort on overcoming the algorithmic challenges imbedded in non-convexity, nonlinearity and non-separability of first- and second- stage variables.

Chapter 3 makes the first attempt to integrate models from both levels. For lower level, a method using finite element (FE) analysis to generate the nonlinear relationship between structural performances of bridges and retrofit levels. This relationship was converted to traffic capacity-cost relationship and used as an input for the upper-level model. Results from the Sioux Falls transportation network demonstrated that the integration of both network and FE modeling for individual structure enhanced the

effectiveness of retrofit strategies, compared to linear traffic capacity-cost estimation and conventional engineering practice which prioritizes bridges according to the severity of expected damages of bridges.

In chapter 4, I develop a minimax regret formulation of network protection problem and integrate with a hazard generation component. At upper level, minimax regret formulation, an alternate way of dealing uncertainty compared to chapter 2, will determine retrofit decisions to use in lower level. The same reformulation technique used in chapter 2 is adopted to reformulate the regret subproblems. The lower level model incorporates a seismic analysis component into the framework such that bridge columns are subject to a set of ground motions. By developing FE models for parameterized retrofit designs, the study captures seismic response of bridge structures. By including a robustness dimension into the bi-level infrastructure system protection framework, the lower level problem will become a simulation based multi-objective optimization which considers cost, safety and robustness. Thereby, a Pareto front can be found in three dimensions and a set of preferred retrofit designs are identified from the Pareto front. Bridge damage scenarios are then generated using the preferred retrofit designs and used as an input of the upper level problem.

Finally, Chapter 5 summarizes the findings in above chapters. An overview of the assumptions and limitations of this work will be included herein, followed by a discussion of future directions that may stem from this dissertation.

Chapter 2 A Mean-Risk MINLP Model for Transportation Network Protection against Disasters

1. Introduction

Many highway bridges in the United States (U.S.), especially old bridges, can be seriously damaged or can collapse even in relatively moderate natural disasters, e.g., earthquakes (Buckle, et al., 2006). In the most recent infrastructure report card issued by the American Society of Civil Engineers (ASCE), one in nine of the bridges in U.S. are deemed structurally deficient(ASCE, 2013). Since 1960's, major structural damage has caused millions of dollars of economic losses in a number of states, including Alaska, California, Washington, and Oregon (Buckle, et al., 2006). To improve this situation, at-risk bridges must be identified and evaluated and retrofitting programs should be in place to strengthen its resilience (Buckle, et al., 2006).

Highway bridge retrofit is one of the most common approaches undertaken to mitigate negative effects of extreme events on highway transportation networks by federal and state departments of transportation. Bridge damages due to extreme events, particularly seismic hazards, may result in direct social and economic losses as a result of post-earthquake bridge repair or restoration, as well as indirect impacts on transportation networks, due to short-term evacuation and emergency response (L. Chang, et al., 2012) and even long-term changes in travel activities (Fan, et al., 2010; C. Liu, et al., 2009).

These adverse impacts can be avoided or alleviated if proactive bridge retrofit strategies are deployed.

The Federal Highway Administration (FHWA) estimates that to eliminate all deficient bridges backlog by 2028, an annual investment of $20.5 billion is needed while currently only $12.8 billion is being spent on. Due to the limited retrofitting resources, it is neither practical nor economical to retrofit all bridges to their full health and a prioritized retrofitting scheme is expected. In practice, an index based bridge retrofit priority has been used, which considers bridge rank, importance, non-seismic deficiencies and network redundancy and prioritizes resources to bridges with higher priority indexes (Buckle, et al., 2006). However, this method may not yield an optimal solution in terms of direct retrofit cost and indirect social losses (e.g., travel delay cost) as this method neglects the effects of networked bridges and consequent redistributions of traffic flows. In other words, damage to one bridge can redistribute vehicular flows over the entire network and affect other at-risk bridges and roadways of the network. It justifies the need to consider bridge retrofitting strategies at a network level.

A network based bridge retrofitting problem is essentially a network design problem (NDP), in which the upper-level problem involves optimal retrofit decisions for best social welfares (e.g., minimum retrofitting cost and travel delay) while lower-level problem accounts for the behaviors of network users which normally presents demand-performance equilibrium (Nagurney, 2006, 2007; Patriksson, 1994; Peeta & Ziliaskopoulos, 2001; Sheffi, 1985). When the problem is under uncertainty, a discrete

set of scenarios is used to approximate uncertainty space. It is unrealistic to consider scenario-specific solutions (policies), since future events are unknown at the time of making decisions and a resulting policy may not even be feasible for other possible scenarios. It is necessary to develop a method that can account for all possible decision-making scenarios. Previous studies use either stochastic programming (SP) (Barbaroso & gcaron, 2004; Fan, et al., 2010; C. Liu, et al., 2009) or robust optimization (RO) method (Atamtürk & Zhang, 2007; H. Sun, et al., 2011; Yafeng, et al., 2009) to take into account all scenarios. In particular, SP takes the expectation of consequences of all scenarios and thus is suitable for problems aiming to achieve long-term economic effects; however, it may have poor performance under extreme events. RO approach, on the other hand, considers worst-case scenario with low occurrence probability, which may lead to too conservative and in most cases costly solutions. A plausible method for bridge retrofit problem should combine the merits of these two stochastic modeling methods to compromise the effects of economics and resilience. In this study, we develop a mean-risk model that considers all scenarios while penalizing worst-case scenarios.

Within our research scope, our study, perhaps, is the first study undertaken in the specific field of transportation network protection specifies the conditional value-at-risk (CVaR) as the risk measure. *CVaR* is not particularly new; it was first introduced by (Andersson, et al., 2001; Rockafellar & Uryasev, 2000, 2002) as a risk assessment technique with wide applications in portfolio management to reduce the probability that a strategy incurs large losses (D. Huang, et al., 2010). In this study, we develop a mean-risk two-stage stochastic programming model. The first-stage decisions indicate the

assignments of retrofit strategies to different bridges in an optimized manner, which are made simultaneously with second-stage traffic assignment decisions with the goal of minimizing the total travel cost where travel time is converted to money value. The *CVaR* at level α is used in the first stage to penalize the worst $1-\alpha$ scenarios with a user-specified confidence level α. The objective is to minimize the total expected direct cost of retrofitting bridges, indirect travel cost and risk consequence by *CVaR*.

Our proposed model is closely related to the risk stochastic model proposed in (C. Liu, et al., 2009), in which a central semi-deviation is identified as the risk measure. However, our study is distinct from this prior study and advances the models in the following aspects. First, the semi-deviation can only capture the effects of scenarios that are worse than the expectation of second stage costs while the *CVaR* is flexible to incorporate a spectrum of scenarios, depending on the pre-defined confidence level and the weighting factors relative to cost terms in the objective. Second, our study relaxes the assumptions of the binary damage states (i.e., either no damage or collapse) and binary retrofit strategies (i.e., retrofit or no retrofit) in the prior study. Although these assumptions help reduce the problem size and consequently the computational challenges associated with solving large-scale problems, this simplification may result in less informative solutions and overestimate costs. In our study, we enrich our model by considering multiple exclusive retrofit strategies and multiple damage states based on a recent study (Y. Huang, et al., 2014). From the modeling perspective, it is not a trivial extension to the prior efforts, due to the inherent correlations between retrofit strategies, damage states, and resulting distributions of traffic flows on the network. In addition, bridge retrofit

strategies are subject to a budget limit, which makes the problem essentially a NP-hard, knapsack problem (Kellerer, et al., 2004).

The mean-risk two-stage stochastic programming model is formulated as a non-convex mixed integer nonlinear programming (MINLP) problem, wherein the bridge capacity is a non-convex nonlinear function of retrofit decisions. In general, it is known that non-convex MINLPs are notoriously difficult to solve (Burer & Letchford, 2012). Thus, another contribution of this study stems from the algorithmic development. In particular, we develop a novel decomposition that is based on the generalized Benders decomposition (GBD) method. Our decomposition resolves the issues of non-separability of first and second stage variables to enable efficient generations of Benders cuts. In this decomposition, we present a convex reformulation of the sub-problem. We justify our model and decomposition method on a hypothetical nine-node network and then apply the model and solution method to solve a stochastic transportation network protection problem based on a benchmark network – the Sioux Falls network (LeBlanc, et al., 1975), and to explore the effects of risk measures and variations in critical parameters on the optimal solutions. The results provide managerial insights for state stakeholders on bridge retrofit schemes.

The remainder of the chapter is organized as follows. A literature review on related topics is presented in section 2. The mean-risk two-stage SP model is presented in section 3, followed by the decomposition in section 4. The numerical results of the two networks

are summarized in section 5. This chapter is concluded in section 6 and the future research is outlined.

2. Literature review

The transportation network protection problems can be grouped into two broad categories, which depend on if bridges are treated as links (L. Chang, et al., 2012; Fan, et al., 2010; C. Liu, et al., 2009) or as paths (Mohaymany & Pirnazar, 2007; Viswanath & Peeta, 2003). The problems based on the links are formulated as maximum capacity or minimum cost flow network design problems with a focus on long-term economic effect of retrofit whereas the studies considering bridges as paths are formulated as maximal covering network design problems, which are more focused on short-term emergency response or maximal coverage of population centers.

Uncertainty is naturally embedded in almost all transportation protection problems. Engineering methods based on the wait-and-see approach (Birge & Louveaux, 2011) seek optimal solutions upon the realizations of uncertainty (or scenario), which are deterministic. The resulting scenario dependent solutions are then aggregated in order to be implemented. Applications of deterministic models are broad for its easy modeling and solutions, for example (Carturan, et al., 2013; L. Chang, et al., 2012; Rokneddin, et al., 2013; Rokneddin, et al., 2011; Zhou, et al., 2010). In contrast to the scenario-dependent deterministic approach, stochastic modeling method yields best anticipative decisions with a consideration of entire uncertainty space. Typical method includes SP

with recourse (Birge & Louveaux, 2011), which is usually in the form of expectation of second-stage cost across all scenarios. Studies based on the SP method are relatively limited compared to the deterministic solution applications, including (Barbaroso & gcaron, 2004; Fan, et al., 2010; C. Liu, et al., 2009). Another stream of research is based on the RO method (Bertsimas & Sim, 2003; Kouvelis & Yu, 1997), which focuses on the worst-case scenario and thus results in more conservative, risk-averse solutions. Its applications include (Atamtürk & Zhang, 2007; Lou, et al., 2009; Yafeng, et al., 2009).

In general, the SP approach may yield solution that is good in a long run perspective, but may perform poorly under certain circumstances of extreme hazardous events, like earthquakes. Though rare, these hazards exert more severe impacts on the system. On other hand, the RO based models may be too conservative to yield any economic solution. Therefore, neither SP approach nor RO based method is best to capture the variability of risk, which motivates this study to seek a new method for economic yet robust solutions. As such, risk measures should be incorporated into decision making process of the SP approach. In particular, we consider *CVaR* as the risk assessment in this study.

In the cost minimization context, value-at-risk (VaR_α) is the α -quantile of the distribution of the cost; that is, it is the smallest value such that the probability of loss exceeds or equals to *VaR* is greater than or equal to a pre-defined confidence level α (Uryasev, 2000). *VaR* can be formulated as a mathematical programming problem. However, it is hard to solve to optimality because *VaR* is non-convex and difficult to optimize numerically for skewed distribution (Uryasev, 2000). Alternatively, *CVaR* is a

risk statistic to measure risk associated with large losses that exceeds *VaR* (Rockafellar & Uryasev, 2000), which has a good mathematical property that preserves convexity (Ahmed, 2006). Particularly, *CVaR* at α level is the expected value of the worst $(1-\alpha)$ of the scenarios (Hong & Liu, 2009). When the confidence level increases, worse scenarios are included so that both the *VaR* and *CVaR* increase, leading to a more risk-averse solution. When all scenarios are considered, the problem is equivalent to a RO problem. This risk measure has been in the past decade broaden up and applied to a number of engineering fields, including electricity operation decision (Yau, et al., 2011), water resources allocation (Shao, et al., 2011), facility location planning for reverse logistics (Toso & Alem, 2014), and hazard material routing (Kwon, 2011). On the other hand, the inherent computational challenges have motivated numerous algorithmic developments. For example, Schultz and Tiedemann (2006) developed a solution algorithm based on Lagrangian relaxation of nonanticipativity to solve a mixed-integer linear program with *CVaR*. Fábián (2008) developed decomposition methods for solving a two-stage SP linear program with *CVaR* and Noyan (2012) extended and solved a similar but two-stage SP mixed-integer linear program for disaster management.

3. The mean-risk two-stage stochastic programming model

Let us denote a transportation network by $G(N, A)$, where N is a set of nodes and A is a set of links on the network. Denote by R and S ($R \subseteq N, S \subseteq N$) the sets of origins and destinations on the network. Denote $\overline{A}$ ($\overline{A} \subset A$), $\left|\overline{A}\right| = \overline{m}$, as the set of arcs that are

subject to seismic hazards, which mainly are the at-risk bridges. The binary decision variable $u_a^h = 1$ if link or bridge a ($a \in \overline{A}$) is retrofitted by strategy h, ($h \in H$), where H is a finite set of applicable retrofit strategies; otherwise $u_a^h = 0$. For an origin-destination (O-D) pair (r, s), we denote by $x^{rs} \in \mathbb{R}_+^m$ the link flow vector and $q^{rs} \in \mathbb{R}_+^n$ the vector of travel demand between an O-D pair. Denote by v_a the total flow on link a. In this model, we allow unsatisfied travel demand post-earthquake for various reasons, such as shutdown of certain roadways, acute increased traffic congestion in the network, etc. The unsatisfied travel demand is captured by decision variable d^{rs} in the model with an imposed penalty cost in the objective function.

In transportation network literature, traffic is often assumed to be in a user-equilibrium condition, where no traveler can further reduce their travel cost by simply changing their own routing decision (Yang & H. Bell, 1998). This assumption holds for a normal situation, where travelers have learned and adapted to daily traffic condition. However, modeling travelers' routing behavior in an environment following extreme events, such as earthquake, is still arguable (Fan, et al., 2010). In this chapter, it is assumed that traffic flow can be controlled to achieve "system optimal" condition and the resulting estimated total cost, the objective value, can be considered as a lower bound of the total cost in reality.

In this study, two sets of probabilistic estimates, including seismic damage to a structure and the probabilities of various earthquake occurrences, are combined to prepare a damage prediction. Let k describe an uncertain event or a scenario. Each

realization with corresponding probability p^k defines a scenario. Let K denote a set of random events, $k \in K$. We assume that if link $a \in \overline{A}$ is retrofitted, the post-earthquake link capacity $\hat{c}_a^k$ is determined by the selected retrofit decision variable $u_a^h = 1$; that is $\hat{c}_a = c_a \sum_{h \in H} u_a^h \theta_a^{h,k}$, where c_a is the link traffic capacity before earthquake, and $\theta_a^{h,k}$ is a parameter describing the post-earthquake link capacity ratio upon receiving retrofit strategy h. Note that only one strategy can be applied to an at-risk bridge, including do-nothing as an option; i.e., $\sum_{h \in H} u_a^h = 1, \ \forall a \in \bar{A}$. The post-earthquake traffic capacity ratio of highway bridge can be determined by using bridge structural assessment (Mackie & Stojadinovic, 2004). For other links ($a \in A \backslash \overline{A}$), the capacities are assumed to be unchanged after earthquakes.

We first present a typical two-stage SP model in a general form in (2-1)-(2-7). The retrofit resource allocation is considered in the first stage of the stochastic program, while the travel cost based on an explicit traffic assignment model is captured in the second stage.

Two-stage stochastic programming model:

$$min_{u \in U} E_{k \in K}\left(f^k(u)\right) = min_{u \in U} c^T u + E_{k \in K}(Q^k(u)) \quad (2\text{-}1)$$

$$s.t. \quad c^T u \leq B \quad (2\text{-}2)$$

$$\sum_{h \in H} u_a^h = 1, \ \forall a \in \bar{A}, \quad (2\text{-}3)$$

$$u \in \{0,1\}^m, \eta \in \mathbb{R}$$

$$Q^k(u) \coloneqq \min_{v,x,d} \gamma[v^T t] + M \sum_{r\in R, s\in S} d^{rs,k} \quad (2\text{-}4)$$

$$Wx^{rs,k} = q^{rs} - d^{rs,k}, \ \ \forall r \in R, s \in S, k \in K \quad (2\text{-}5)$$

$$v_a^k = \sum_{r\in R} \sum_{s\in S} x_a^{rs,k}, \ \ \forall a \in A, k \in K \quad (2\text{-}6)$$

$$t(u, v_a) = t_0[1 + \beta(\frac{v_a}{\hat{c}_a^k})^4], \forall a \in A, \quad (2\text{-}7)$$

with $$\hat{c}_a^k = \begin{cases} \sum_{h\in H} u_a^h \theta_a^{h,k} c_a, \forall a \in \bar{A} \\ c_a, \forall a \in A \backslash \bar{A} \end{cases}, \forall k \in K$$

$$x^{rs,k} \geq 0, \ \ \forall r \in R, s \in S, k \in K$$

$$v_a^k \geq 0, \ \ \forall a \in A, k \in K$$

$$d^{rs,k} \geq 0, \ \ \forall r \in R, s \in S, k \in K$$

The objective (2-1) is to minimize the total expected system cost. Here $f^k(u) = c^T u + Q^k(u)$ is the total cost function for scenario k, which consists of first stage cost $c^T u$ and recourse function $Q^k(u)$. The recourse function encompasses the travel cost and the penalty cost of unsatisfied demand $d^{rs,k}$. Constraint (2-2) is the budget constraint. c is the cost vector for all bridges and retrofit alternatives, B is the total retrofit budget. Constraints (2-3) require that for each bridge receive only one retrofit strategy. Recourse function is defined in equation (2-4), in which v is a vector of link flow v_a^k for link a scenario k, γ is a parameter that converts travel time to money value, and M is the penalty

for the unsatisfied demand $d^{rs,k}$. Constraint set (2-5) assures travel demand is satisfied or penalized, where W is a node-link adjacency matrix. Constraints (2-6) describe the relationship between the total link flow v_a^k and link flow $x_a^{rs,k}$ for each O-D pair rs. The equation set (2-7) describes the travel time based on a non-decreasing link performance function - the Bureau of Public Roads (BPR) function. The travel time relates to link flow v and post-earthquake link capacity. Note that as the post-earthquake link capacity is a result of retrofit decisions, the decision variable u appears on the denominator of the travel time cost function, which results in the non-convexity and nonlinearity.

Observation 1. The general problem (2-1)-(2-7) has relatively complete recourse, i.e., subproblem (2-4)-(2-7) is feasible for every $u \in U$.

By definition, a stochastic program has relatively complete recourse if every feasible first-stage solution u satisfies the second-stage problem (Birge & Louveaux, 2011). In our problem, all travel demand is satisfied (or penalized for economic concerns) in the second stage regardless of the retrofit decisions made in the first stage.

We now turn to introducing our mean-risk MINLP model, which combines the two-stage SP model and the *CVaR* as the risk assessment. The *CVaR* can be expressed as below:

$$CVaR_\alpha(Y) := E(Y : Y \geq VaR_\alpha(Y)).$$

For a finite probability space *K*, the objective function of a mean-risk two-stage stochastic program is defined as:

$$min_{u\in U} E\left(f^k(u)\right) + \lambda CVaR_\alpha(f^k(u)),$$

where λ is the tradeoff coefficient associated with the ratio of the total expected cost $E\left(f^k(u)\right)$ to the risk term $CVaR_\alpha(f^k(u))$. Via simple manipulation arising out of translation invariance of *CVaR* (Noyan, 2012), the mean-risk two-stage SP program is equivalent to the following program (2-8):

Mean-risk two-stage stochastic programming model:

$$\min_{u\in U}(1+\lambda)c^T u + E(Q^k(u)) + \lambda(\eta + \tfrac{1}{1-\alpha}E([Q^k(u)-\eta]^+)) \qquad (8)$$

s.t. constraints (2)-(7).

where η is the value-at-risk, $\eta \in \mathbb{R}$, and $[z]^+ = \max\{0, z\}, \forall z \in \mathbb{R}$.

The objective is to minimize the total cost of retrofitting bridges, expected travel cost, and risk consequence ($CVaR$). λ is a pre-defined weighting factor. A larger λ value leans towards *CVaR*, which weighs more on scenarios with worse consequences, and thus results in a more conservative solution. On the other hand, a smaller λ value yields a solution that weighs more on the expected cost, and thus the solution is more risk neutral.

Our mean-risk two-state model yields a *non-convex* MINLP due to the following reasons:

(a) bilinear expression $v^T t$ in the objective function (2-5) for $Q^k(u)$,

(b) nonlinear equality constraints (2-7), and

(c) fractional function $\frac{v_a}{\hat{c}_a^k}$ in (2-7).

For large-scale instances, this non-convex MINLP is intractable with off-the-shelf MINLP solvers. As illustrated in section 5.1, the poor performance even on a simple nine-node network motivates our algorithmic development as discussed in section 4.

4. Decomposition methods

Extensive algorithmic efforts have been made to improve the solution efficiency of MINLPs, including the widely used branch and bound (Gupta & Ravindran, 1985) with its variants - LP/NLP based branch and bound method (Quesada & Grossmann, 1992) and spatial branch and bound (Smith & Pantelides, 1999), and Generalized Benders Decomposition (GBD) method (Geoffrion, 1972). The branch and bound method is essentially an implicit enumeration procedure, which can be computationally expensive when the number of integer variables is large. The GBD on the other hand is effective in handling large-scale problem by decomposing intractable MINLP to tractable sub-problems for improved solution efficiency. In this study, we develop a decomposition

method based on GBD. Also note that there are other plausible solution methods, including Extended Cutting Plane method (Westerlund & Pettersson, 1995), and outer approximation (Duran & Grossmann, 1986). Comparisons between these different methods in terms of solution quality and performance are worth investigations in future works.

The model (2-8) will be decomposed into a master and sub-problems. The master problem is a mixed integer linear program and contains first-stage integer variables u and the value-at-risk η. The sub-problems are evaluated for travel cost and CVaR at the optimum of the master problem. We will discuss the details on decomposition method in this section.

4.1 The generalized Benders decomposition method

The Benders decomposition method (Benders, 1962) was designed to solve mix-integer linear problems, which was later generalized to solve nonlinear problems (Geoffrion, 1972), also known as GBD. When complicating variables are temporally held fixed, the method can render the remaining optimization problem that is considerably more tractable. As for this study, if bridge retrofit decision variable u and the value-at-risk η, are temporarily fixed, the remaining problem (2-5) – (2-7) becomes a traffic assignment problem based on system-optimization condition, which may be effectively solved by using commercial non-linear program solvers, such as CONOPT (Drud, 1994).

The CVaR value can be obtained by aggregating travel cost function values from the traffic assignment problems corresponding to different scenarios.

Overview of GBD. We first illustrate how GBD works in a general way, followed by the development of this method for application to our problem in great details. GBD decomposes a problem into two parts by projecting the original problem onto the space of complicating variables. Let us take the following general optimization problem as an example:

$$min_{u,x} f_1(u) + f_2(u,x), \quad s.t. G(x,u) \leq 0, x \in X, u \in \{0,1\}^m \tag{2-9}$$

Assume that $f_1(u)$ and $G(x,u)$ are both convex functions and that X is a non-empty convex set. Let vector u be the complicating variables and U be the decision space for u. Assume that $f_2(u,x)$ is a non-convex program on u and x jointly; however, fixing u will render it convexity in x. The projection of model (2-9) onto u space is completed as (2-10) and (2-11),

$$min_u f_1(u) + v(u), \ \ s.t. \ u \in U \cap V \tag{2-10}$$

where

$$v(u) = inf_x[f_2(u,x)], \quad s.t. G(u,x) \leq 0, x \in X \tag{2-11}$$

and

$$V = \{u | G(u,x) \leq 0, for \ some \ x \in X\},$$

Note that V is the set of induced constraints, which assures that $v(u)$ is feasible. Set V is a convex set since it is a projection of a convex set. The $v(u)$ is the optimal value of $f_2(u,x)$ for a fixed u; in other words, it is the objective value of the optimization problem parameterized by u. The function $v(u)$ is convex as $f_2(u,x)$ is convex in x for a fixed u. By designation of u as complicating variables, evaluating $v(u)$ is much easier than solving problem (2-9).

According to Theorem 2.1 in (Geoffrion, 1972), if (u^*, x^*) is optimal in (2-9), then u^* must be optimal in (2-10); If u^* is optimal in (2-10) and x^* achieves the infimum in (2-11) with $u = u^*$, then (u^*, x^*) is optimal in (9).

Thus, problems (2-9) and (2-10)-(2-11) are equivalent and (2-10)-(2-11) can in turn be re-written as

$$min_{u,\phi} f_1(u) + \phi, s.t. \phi \geq v(u), u \in U \cap V, \qquad (2\text{-}12)$$

Problem (2-12) is equivalent to problem (2-9) and can be solved by using cutting-plane methods to approximate the convex set V and convex function $v(u)$.

Here, we will demonstrate how to use Lagrangian function to form *master* and *sub-problems*. The function $v(u)$ in (2-10)-(2-11) is the *sub-problem* and according to strong duality theory it can be written as,

$v(u) = [inf_x[f_2(u,x)], s.t. G(u,x) \leq 0, x \in X] = \left[sup_{\mu \geq 0}[inf_{x \in X} L(u,x,\mu)]\right], \forall u \in U \cap V,$

where $L(u,x,\mu) = f_2(u,x) + \mu^T G(u,x)$, is the Lagrangian function. With a scalar ϕ, the master problem is:

$$min_{u\in U,\phi} f_1(u) + \phi, \text{ s.t. } \phi \geq inf_{x\in X}\, L(u,x,\mu), \forall \mu \geq 0$$

Based on GBD, we decompose our mean-risk model in (8) into master problem described in (2-13) – (2-15) and sub-problems to approximate travel cost function $Q^k(u)$ in (2-16).

Master problem:

$$\text{mininimize } (1+\lambda)c^T u + \phi_1 + \lambda\phi_2\,,\ u \in U \tag{13}$$

where

$$U \coloneqq \{u | u \in \{0,1\}^m, c^T u \leq B,\ \textstyle\sum_{h\in H} u_a^h = 1,\ \ \forall a \in \bar{A}\}$$

s.t.

optimality cut 1*:* $\phi_1 \geq \sum_k p^k Q^k(u)$ (14)

optimality cut 2*:* $\phi_2 \geq \eta + \frac{1}{1-\alpha}\sum_k p^k\,[Q^k(u) - \eta]^+$ (15)

In the objective function (2-13), the recourse function travel cost and *CVaR* are not known explicitly in advance. Thus, the optimality cuts (2-14) and (2-15) are added to approximate them. As per Observation 1 in section 3, this problem has *relatively complete recourse* and the feasibility cut constraint can thus be omitted. Let $\overline{u}$, $\bar{\phi}_1$, and

$\bar{\phi}_2$ be the optimal solutions to the master problem. Then each subproblem is solved at the optimum of the master problem.

Sub-problem $Q^k(\bar{u})$, $k \in K$:

$$min_{v,x,d} Q^k(\bar{u}) = min_{v,x,d} \gamma[v^T t] + M \sum_{r\in R, s\in S} d^{rs,k} \quad (2\text{-}16)$$

s.t. constraints (2-5) – (2-7)

If $\bar{\phi}_1 < \sum_k p^k Q^k(\bar{u})$, the optimality cut (2-14) will be added to the master problem. Similarly, if $\bar{\phi}_2 < \eta + \frac{1}{1-\alpha}\sum_k p^k [Q^k(\bar{u}) - \eta]^+$, the optimality cut (2-15) will be added to the master problem.

Proposition 1. For every $u \in U, \mathrm{k} \in K$, the subproblem for $Q^k(u)$ is a convex minimization problem.

Proof. For a fixed $\bar{u}$, $\hat{c}_a^k$ is a parameter. For $x, v, d \geq 0$, v_a^k, $\frac{(v_a^k)^5}{(\hat{c}_a^k)^4}$ and $d^{rs,k}$ are all convex functions. The objective function (2-16), as a summation of these convex functions, is convex. With constraint sets (2-5) and (2-6) being affine, the sub-problem for $Q^k(u)$ is a convex minimization problem. A lower bound for sub-problem $Q^k(u)$can be obtained when the transportation network is intact. □

The function $Q^k(u)$, as stated, is the *value function* of a convex optimization problem where the dependence on *u* is through the denominator of the objective in (2-16). Due to this non-separability between *u* and the second-stage variables, it is unclear whether $Q^k(u)$ is a convex or a non-convex function. We will exploit the structure of the set *U* and use a reformulation trick to show in subsection 4.2 that $Q^k(u)$ is convex in *u*.

4.2 Reformulation of recourse function

The reformulation is completed in two steps. First, we eliminate complicating variables in the denominator of BPR function by substituting it with a new variable. Second, by using logic constraints, we make the formulation linear separable in first and second stage variables. The details on the reformulation are discussed in this section.

We first introduce a new, non-negative continuous variable y_a^k as:

$$y_a^k \geq \frac{(v_a^k)^5}{\left[c_a \sum_{h\in H} u_a^h \theta_a^{h,k}\right]^4}, \forall a \in \overline{A}. \tag{2-17}$$

Note that this inequality only applies to at-risk bridges. We assume that the poster-disaster capacities of other road links remain unchanged. Through simple manipulations, we obtain the inequality set (18):

$$(v_a^k)^5 \leq y_a^k \left[\sum_{h\in H} u_a^h \theta_a^{h,k} c_a\right]^4, \forall a \in \bar{A} \tag{2-18}$$

Remark 1. Since $\sum_{h\in H} u_a^h = 1, \forall a \in \bar{A}$, and $u \in \{0,1\}^{|H|}$, then $(u_a^h)^n = (u_a^h),\ \forall h \in H, n = 1,2,\ldots$ and $u_a^{h_1} \times u_a^{h_2} = 0, if\ h_1 \neq h_2, \forall h_1, h_2 \in H$.

Based on Remark 1, inequality set (2-18) is equivalent to

$$(v_a^k)^5 \leq y_a^k[\sum_{h\in H} u_a^h\,(\theta_a^{h,k})^4]c_a^4, \forall a \in \bar{A} \tag{2-19}$$

To apply GBD to generate optimality cuts, this inequality set should be linearly separable in the first-stage variable vector u and second-stage variable vector y. We introduce another non-negative continuous variable $z_a^{h,k}$ and let $z_a^{h,k} = y_a^k u_a^h$. Then the following equivalency holds.

Proposition 2. Inequality set (19) is equivalent to the system of inequalities (2-20) – (2-22)

$$(v_a^k)^5 \leq \sum_h z_a^{h,k}\left(\theta_a^{h,k}\right)^4 c_a^4, \forall a \in \bar{A}, k \in K \tag{2-20}$$

$$z_a^{h,k} \leq \frac{(\bar{v}_a)^5}{\left(\theta_a^{h,k}\right)^4 c_a^4} u_a^h, \forall a \in \bar{A}, h \in H, k \in K \tag{2-21}$$

$$y_a^k = \sum_h z_a^{h,k}, \forall a \in \bar{A}, k \in K \tag{2-22}$$

where $\bar{v}_a = \alpha c_a$ is the upper-bound traffic volume of link a, and α is a sufficiently large number.

Proof: Let $\overline{y}_a^k := \frac{(\bar{v}_a)^5}{\sum_{h\in H}\left(c_a\theta_a^{h,k}\right)^4 u_a^h}$. For every $a \in \bar{A}$ and $u \in U$, the equation $\frac{1}{\sum_{h\in H}\left(c_a\theta_a^{h,k}\right)^4 u_a^h} = \sum_{h\in H}\frac{u_a^h}{\left(c_a\theta_a^{h,k}\right)^4}$ holds. It follows that $\overline{y}_a^k = \frac{(\bar{v}_a)^5}{c_a^4}\sum_{h\in H}\frac{u_a^h}{\left(\theta_a^{h,k}\right)^4}$. Based on Remark 1, $\overline{y}_a^k u_a^h = \frac{(\bar{v}_a)^5}{c_a^4}\frac{u_a^h}{\left(\theta_a^{h,k}\right)^4}$ is valid. Thus constraint set (2-21) is equivalent to the following inequality:

$$z_a^{h,k} \le \overline{y}_a^k u_a^h, \forall a \in \bar{A}, h \in H, k \in K. \qquad \text{(2-21')}$$

Consider a solution (v_a^k, y_a^k, u_a^h) that satisfies inequality set (19), then the inequalities $(v_a^k)^5 \le y_a^k\left[\sum_{h\in H} u_a^h\left(\theta_a^{h,k}\right)^4\right]c_a^4$ and $z_a^{h,k} \le y_a^k u_a^h$ hold. Since $z_a^{h,k} = y_a^k u_a^h$, one obtains inequality (2-20): $(v_a^k)^5 \le \sum_h z_a^{h,k}\left(\theta_a^{h,k}\right)^4 c_a^4$. The inequality (2-21') $z_a^{h,k} \le \overline{y}_a^k u_a^h$ holds, as $\overline{y}_a^k$ is the upper bound of y_a^k. Since $\sum_{h\in H} u_a^h = 1$ and $u_a^h \in \{0,1\}$, one can obtain $\sum_h z_a^{h,k} = \sum_h u_a^h y_a^k = y_a^k \sum_h u_a^h = y_a^k$, which is (2-22).

On the other hand, assume that a solution $(v_a^k, y_a^k, u_a^h, z_a^{h,k})$ satisfies (2-20), (2-21') and (2-22).

Since $\sum_{h\in H} u_a^h = 1$ and $u_a^h \in \{0,1\}$, for $\forall a \in \bar{A}$, $\forall k \in K$, there is a $h = h^*$ such that $u_a^{h^*} = 1$ and $u_a^h = 0$, if $h \ne h^*$. $z_a^{h,k} = y_a^k u_a^h$ is equivalent to

$$\begin{cases} z_a^{h,k} = y_a^k, & for\ h = h^* \\ z_a^{h,k} = 0, & for\ h \neq h^* \end{cases}'$$

From (2-21'), one can obtain $z_a^{h,k} = 0, \text{if } h \neq h^*$. From (2-24), $z_a^{h^*,k} = y_a^k$. Therefore, (2-21') and (2-22) is equivalent to $z_a^{h,k} = y_a^k u_a^h$. By substituting $z_a^{h,k}$ for $y_a^k u_a^h$ in inequalities (2-20), inequalities (2-19) hold. □

According to **proposition 2**, $Q^k(u)$ is equivalent to (2-23) and (2-24) for each $k \in K$.

$$Q^k(u) = inf_{x,y,z,v}[f_2^k(u,(x,y,z,v))] \tag{2-23}$$

$$s.t. \quad G^k(z,u) \leq 0 \tag{2-24}$$

$$(x,y,z,v) \in X^k,$$

$$u \in U$$

where

$G^k(z,u)$ has $|\overline{A}| \times |H|$ components:

$G_a^{h,k}(z,u) = z_a^{h,k} - \overline{y}u_a^h, \forall h \in H$, and

$\overline{y} = \max\{\overline{y}_a^k, \forall a \in \bar{A}, \forall k \in K\}$.

$X^k \coloneqq \{(x,y,z,v) | Wx^{rs,k} = q^{rs} - d^{rs,k}, \forall r \in R, s \in S$

$$v_a^k = \sum_{r \in R} \sum_{s \in S} x_a^{rs,k}, \forall a \in A$$

$$(v_a^k)^5 \leq \sum_h z_a^{h,k} \left(\theta_a^{h,k}\right)^4 (c_a)^4 \,, \forall a \in A$$

$$z_a^{h,k} = \sum_k y_a^k \,, \forall a \in \bar{A}, h \in H\}, \text{ and}$$

$$U \coloneqq \{u | u \in \{0,1\}^m, c^T u \leq B,\ \sum_{h \in H} u_a^h = 1,\ \ \forall a \in \bar{A}\}.$$

Let $\mu \geq 0$ be the dual variable vector associated with (2-24). Convexity of the subproblem and strong duality theory imply that $\forall u \in U$, we have,

$$Q^k(u) = sup_{\mu \geq 0} \left[inf_{x \in X} [f_2\big(u, (x, y, z, v)\big) + \mu^T G^k(z, u)]\right] \qquad (2\text{-}25)$$

Proposition 3. $Q^k(u)$ is a convex function in u.

Proof: Proposition 2 makes the sub-problem separable in the first and second-stage variables. Since subproblem is convex in second-stage variables, strong duality implies $Q^k(u)$ is convex. □

The sub-problem is solved at the optimum of master problem $\bar{u}$ and the optimal value $Q^k(\bar{u})$ is attained in (2-25) for scenario *k*, resulting in a Lagrangian multiplier μ^k.

$$Q^k(\bar{u}) = inf_{(x,y,z,v) \in X}\, t_0 \sum_{a \in \bar{A}} (v_a^k + \beta y_a^k) + t_0 \sum_{a \in \bar{A}} v_a^k \left(1 + \beta \left(\frac{v_a^k}{c_a}\right)^4\right) + (\mu^{kl})^T (z - \overline{y}\bar{u})$$

$$= -\overline{y}(\mu^k)^T\bar{u} + inf_{(x,y,z,v)\in X}\left[t_0\sum_{a\in\bar{A}}(v_a^k + \beta y_a^k) + t_0\sum_{a\in A\setminus\bar{A}} v_a^k\left(1 + \beta\left(\frac{v_a^k}{c_a}\right)^4\right) + (\mu^k)^T z\right] \quad (2\text{-}26)$$

Proposition 4. Let $\bar{u}^l$ be the optimum solution of the master problem at l^{th} iteration. Then the optimality cuts for the l^{th} iteration are:

$$\phi_1 \geq \sum_k p^k(Q^k(\bar{u}^l) - \mu^{kl}\overline{y}(u - \bar{u}^l)) \quad (2\text{-}27)$$

$$\phi_2 \geq \eta + \frac{1}{1-\alpha}\sum_k p^k\xi^k \quad (2\text{-}28)$$

$$\xi^k \geq Q^k(\bar{u}^l) - \mu^{kl}\overline{y}(u - \bar{u}^l) - \eta,\ \forall k \in K \quad (2\text{-}29)$$

$$\xi^k \geq 0,\ \forall k \in K. \quad (2\text{-}30)$$

Proof: From (2-14):

$$\phi_1 \geq \sum_k p^k\left(\inf_{(x,y,z,v)\in X}\left[f_2\left(u,(x,y,z,v)\right) + \mu^{kl}G(z,u)\right]\right)$$

$$= \sum_k p^k\left(\inf_{(x,y,z,v)\in X} t_0\sum_{a\in\bar{A}}(v_a^k + \beta y_a^k) + t_0\sum_{a\in\bar{A}} v_a^k\left(1 + \beta\left(\frac{v_a^k}{c_a}\right)^4\right) + (\mu^{kl})^T(z - \overline{y}\bar{u})\right)$$

$$= \sum_k p^k \left(-\overline{y}(\mu^{kl})^T \bar{u}^l + inf_{(x,y,z,v)\in X}\left[t_0 \sum_{a\in\bar{A}}(v_a^k + \beta y_a^k) + t_0 \sum_{a\in A\setminus\bar{A}} v_a^k \left(1 + \beta\left(\frac{v_a^k}{c_a}\right)^4\right) + (\mu^k)^T z\right]\right.$$

By substitution of $Q^k(\bar{u}^l)$ in (2-26), one can obtain (2-27).

Similarly, from (2-15) and (2-26):

$$\phi_2 \geq \eta + \frac{1}{1-\alpha}\sum_k p^k \left(\inf_{(x,y,z,v)\in X}\left[f_2\left(u,(x,y,z,v)\right) + \mu^{kl}G(z,u) - \eta\right]^+\right)$$

$$= \eta + \frac{1}{1-\alpha}\sum_k p^k \left(\inf_{(x,y,z,v)\in X}\left[t_0 \sum_{a\in\bar{A}}(v_a^k + \beta y_a^k) + t_0 \sum_{a\in A\setminus\bar{A}} v_a^k \left(1 + \beta\left(\frac{v_a^k}{c_a}\right)^4\right)\right] + (\mu^{kl})^T[(z - \overline{y}\bar{u}^l) - \eta]^+\right)$$

$$= \eta + \frac{1}{1-\alpha}\sum_k p^k \left(-\overline{y}(\mu^{kl})^T \bar{u}^l + \inf_{(x,y,z,v)\in X}\left[t_0 \sum_{a\in\bar{A}}(v_a^k + \beta y_a^k) + t_0 \sum_{a\in A\setminus\bar{A}} v_a^k \left(1 + \beta\left(\frac{v_a^k}{c_a}\right)^4\right)\right] + (\mu^{kl})^T[z - \eta]^+\right)$$

one can obtain (2-28)-(2-30). □

For a better convergence, another optimality cut is added to improve the global lower bound of $Q^k(u)$. For a given $\bar{u}^l \in \{0,1\}^{|\bar{A}|\times|H|}$, define $S(\bar{u}^l) \coloneqq \{i|\bar{u}_i^l = 1\}$ and the integer optimality cut (Laporte & Louveaux, 1993) at $\bar{u}^l$ is

$$\phi_1 \geq (\sum_k p^k Q^k(\bar{u}^l) - Q^L)\left(\sum_{i\in S(\bar{u}^l)} u_i - \sum_{i\notin S(\bar{u}^l)} u_i - |S(\bar{u}^l)|\right) + \sum_k p^k Q^k(\bar{u}^l), \quad (2\text{-}31)$$

where $Q^L \in \mathbb{R}$ is the lower bound on $Q^k(u), \forall k, u$, which can be obtained: $Q^L = \min_{k\in K}\{\gamma[v^T t] + M\sum_{r\in R, s\in S} d^{rs,k}\}$. Note that because $\sum_k p^k = 1$, Q^L is also a lower bound on $\sum_k p^k Q^k(u)$.

Multiple optimality cuts may help improve algorithm efficiency. Readers may refer to (Birge & Louveaux, 1988) for details. The corresponding multi-cuts for (2-27) and (2-31) are (2-32) and (2-33).

$$\phi_1^k \geq Q^k(\bar{u}^l) - \mu^{kl}\overline{y}(u - \bar{u}^l) \quad (2\text{-}32)$$

$$\sum_k p^k(\phi_1^k) \geq \left(\sum_k p^k Q^k(\bar{u}^l) - Q^L\right)\left(\sum_{i\in S(\bar{u}^l)} u_i - \sum_{i\notin S(\bar{u}^l)} u_i - |S(\bar{u}^l)|\right) + \sum_k p^k Q^k(\bar{u}^l) \quad (2\text{-}33)$$

Accordingly, we should use the aggregation of cuts $\sum_k p^k(\phi_1^k)$ to replace ϕ_1 in the objective function of master problem (2-13). Note that due to the *CVaR* function definition, optimality cuts (2-28)-(2-30) are already in multi-cut version. In each iteration, there are $|K| + 1$ constraints added to the master problem, consisting of $|K|$ constraints (2-29) and one constraint (2-28).

The decomposition algorithm procedure:

Step 1: Initialization $l = 0$

Step 2: Solve master problem (2-13)-(2-15)

Let $(\overline{u}, \overline{\phi}_1, \overline{\phi}_2)$ be optimal solution, then$\overline{\phi} = \overline{\phi}_1 + \lambda\overline{\phi}_2$

Step 3: Solve the sub-problems (2-16), (2-18) for all scenarios. Set $l = l + 1$:

Calculate $\phi^* = \sum_k p^k Q^k(\overline{u}) + \lambda CVaR(\overline{u})$.

Step 4: The procedure terminates if the optimality gap $|1 - \frac{\overline{\phi}}{\phi^*}| \leq \varepsilon$ (ε is a predefined small value) is met. Optimal solution is found. Otherwise, add optimality cuts (2-27)-(2-30) (or the multi-cut version (2-32)-(2-33)) and cuts (2-28)-(2-30) to the master problem, and go back to step 2.

5. Numerical examples

The proposed mean-risk model and decomposition methods are first justified using a small nine-node hypothetical network. A well-known Sioux-Falls network (LeBlanc, et al., 1975) is then used to explore the impacts of uncertainty, network topology, and critical parameters on the strategic decisions on highway bridge retrofits. All numerical implementations run on a desktop with 8 GB RAM and Intel Core i5-2500@3.40GHz

processor under Windows 7 environment. Note that all algorithm implementations in this study stop at $\varepsilon = 1\%$.

5.1 Nine-node network

The network is shown in Figure 2.1, which consists of nine nodes, 24 directional links, and 72 (= 8×9) O-D pairs. Assume that three bridges on both directions on the network, labeled as A, B, and C, are vulnerable to seismic disasters and their poster-disaster capacities may be reduced while other road links are assumed intact.

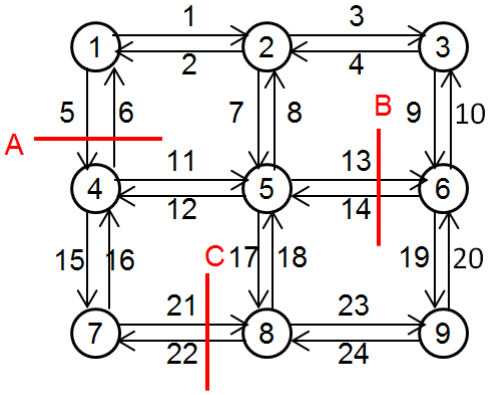

Figure 2.1 Nine-node network

The bridge post-earthquake capacity ratio $\theta_a^{h,k}$ depends on the specific scenario, location of the bridge, and the retrofit strategy applied. The $\theta_a^{h,k}$ is based on the structural performances and retrofit strategies (Mackie & Stojadinovic, 2004). There are five

strategies considered, as shown in Table 2.1, including "do nothing" h0 strategy (Y. Huang, et al., 2014). A higher numbered strategy indicates a more robust yet more costly strategy, and vice versa. In this numerical experiment, the values are randomly generated. For demonstration purpose, Table 2.1 shows such values for only one scenario and there are as many such tables as the number of scenarios. Other critical parameters are: $= 0.7, \beta = 0.15, \gamma = 1000, \lambda = 1$, and $\overline{y} = 1000$.

Table 2.1 θ values of a scenario (k)

Link	Strategy				
	h0	h1	h2	h3	h4
link5	0.05	0.5	0.5	0.5	1
link6	0.05	0.5	0.5	0.5	1
link13	0.5	0.5	0.5	0.75	0.75
link14	0.5	0.5	0.5	0.75	0.75
link21	0.17	0.33	0.33	0.67	0.67
link22	0.17	0.33	0.33	0.67	0.67

To justify the decomposition method, we need obtain benchmark solutions, such as from commercial solver BONMIN (Bonami, et al., 2008), which however is a convex MINLP solver. Thus we first convexify the non-convex MINLP in (2-8) as the program presented in (2-34) – (2-37).

$$\min_{u,\eta,z,v,x,d,y,w}(1+\lambda)c^T u + \lambda\eta + \sum_{k\in K} p^k \left(M \sum_{r\in R, s\in S} d^{rs,k} + \frac{\lambda}{1-\alpha}\xi^k\right) +$$

$$\gamma t_0 \sum_{k\in K} p^k \left(\sum_{a\in \bar{A}}\left[v_a^k + \beta \sum_{h\in H} w_a^{h,k}\right] + \sum_{a\in A\setminus\bar{A}}\left[v_a^k + \beta \frac{(v_a^k)^5}{c_a^4}\right]\right) \quad (2\text{-}34)$$

$s.t.$ Constraints (2-4) and (2-6)

$$\xi^k \geq \gamma t_0 \left(\sum_{a\in \bar{A}}\left[v_a^k + \beta \sum_{h\in H} w_a^{h,k}\right] + \sum_{a\in A\setminus\bar{A}}\left[v_a^k + \beta \frac{(v_a^k)^5}{c_a^4}\right]\right) +$$

$$M \sum_{r\in R, s\in S} d^{rs,k} - \eta, \ \forall k \in K \quad (2\text{-}35)$$

$$(v_a^k)^5 \leq \sum_{h\in H}\left(c_a \theta_a^{h,k}\right)^4 z_a^{h,k}, \forall a \in \bar{A}, k \in K \quad (2\text{-}36)$$

$$z_a^{h,k} \leq \bar{y}_a^k u_a^h, \forall h \in H, a \in \bar{A}, k \in K \quad (2\text{-}37)$$

$$\xi, v, x, d, z \geq 0$$

In particular, we test the model using four different sizes of scenario sets. In each set, scenarios are randomly generated to create variations in uncertainty realizations in order to justify the effects of *CVaR*. The sum of the probabilities of the scenarios in a set equals one. We found that the optimal objective values obtained from BONMIN and GBD are identical for all scenario sets. In addition, we compare the computing times and report the GBD iterations in Table 2.2. From the results, the computing times by using GBD are substantially lower than the BONMIN in all cases. The numerical results give us confidence in accepting the GBD as an effective solution method. Note also that solving times rise with the increase of number of scenarios, although it does not necessarily translate to a higher number of GBD iterations. This is because sub-problems become

more difficult to solve with more scenarios, which results in longer solving time per iteration. This explains why GBD results in almost identical solving time in the case of 24 scenarios as in the case of 18 scenarios even though GBD finishes with fewer iterations in the case of 24 scenarios.

Table 2.2 Comparisons between GBD and exact solutions

Number of scenarios	Obj. value (106)		CPU seconds		GBD iterations
	BONMIN	GBD	BONMIN	GBD	
6	466.416	466.416	44	7	15
12	465.074	466.144	121	21	29
18	462.618	462.063	237	21	21
24	460.483	460.484	323	22	18

5.2 Sioux Falls network

The Sioux Falls network as shown in Figure 2 consists of 24 nodes, 76 links, and 552 O-D pairs. The trip demands between all O-D demands are adopted from (LeBlanc, et al., 1975). Assume that there are four bridges, labeled as A, B, C, and D, vulnerable to seismic hazards. We adopted critical parameters from (Fan, et al., 2010), including $\beta = 0.15$, and the peak 2-hour conversion value $\gamma = 2400$ to convert peak 2-hour delay to a monthly monetary value loss, which is set as $8 \times 30 \times 10 = 2400$, where 8 is daily adjust factor, with 30 days duration, and 10 is value of travel time savings for drivers.

Traditional engineering method estimates earthquake damage of structures using discrete damage states (Choi, et al., 2004) , that is, the residual post-earthquake capacity ratio $\theta_{\mathrm{a}}^{\mathrm{h,k}}$, have discrete values. Note that there are possible noises in estimating the post-earthquake traffic capacity for each structure. Without any existing data from the structure assessment, we randomly generate $\theta_{\mathrm{a}}^{\mathrm{h,k}}$ such that there are substantial variations among different scenarios to justify the use of stochastic programming method in our study. The random $\theta_{\mathrm{a}}^{\mathrm{h,k}}$, are generated following the two steps. First, a list of discrete numbers are created: $\{\hat{\theta}_n \coloneqq \frac{n}{N}, n = 1, \dots, N\}$, from which the $\theta_{\mathrm{a}}^{\mathrm{h,k}}$ will be assigned. The number N is user-defined (e.g., 6 in this study). For a given bridge a under scenario k, the $\theta_{\mathrm{a}}^{\mathrm{h,k}}$ value should be nondecreasing with increasingly enhanced strategy h (i.e., higher numbered strategies), such as $\theta_{\mathrm{a}}^{\mathrm{h4,k}} \geq \theta_{\mathrm{a}}^{\mathrm{h3,k}}$. Second, when generating the $\theta_{\mathrm{a}}^{\mathrm{h,k}}$ for different scenarios k, we intend to further increase the variations among different scenarios by differentiating three categories of scenarios: the low-, median- and high-damage scenarios. The higher damage is, the lower $\theta_{\mathrm{a}}^{\mathrm{h,k}}$ will be. In particular, we use the following simple mechanism to differentiate the $\theta_{\mathrm{a}}^{\mathrm{h,k}}$ values as: $\{\theta_{\mathrm{n}}^{low} \coloneqq \frac{n}{N}, n = 1, \dots, N\}$, $\{\theta_{\mathrm{n}}^{median} \coloneqq \frac{n}{N}, n = 1, \dots, N-1\}$, and $\{\theta_{\mathrm{n}}^{high} \coloneqq \frac{n}{N}, n = 1, \dots, N-2\}$, for low-, median- and high-damage scenarios, respectively. Further, we specify the occurrences of the three categories of scenarios following a predefined ratio, such as 5:3:2 for low-, median- and high-damage scenarios, respectively. For example, for a total of 20 scenarios, the low-, median- and high-damage scenarios are 10, 6, and 4, respectively.

We adopt the same five-strategy scheme and initial point settings from the nine-node network example. There are total 534,101 variables including 40 binary variables and 168,041 constraints. BONMIN fails to find an integer solution within eight CPU hours. The results of the Sioux Falls network are thus obtained by using decomposition method. In this section, we aim to explore the impacts of uncertainty, network topology, and critical parameters on the retrofit strategies using the Sioux Falls network.

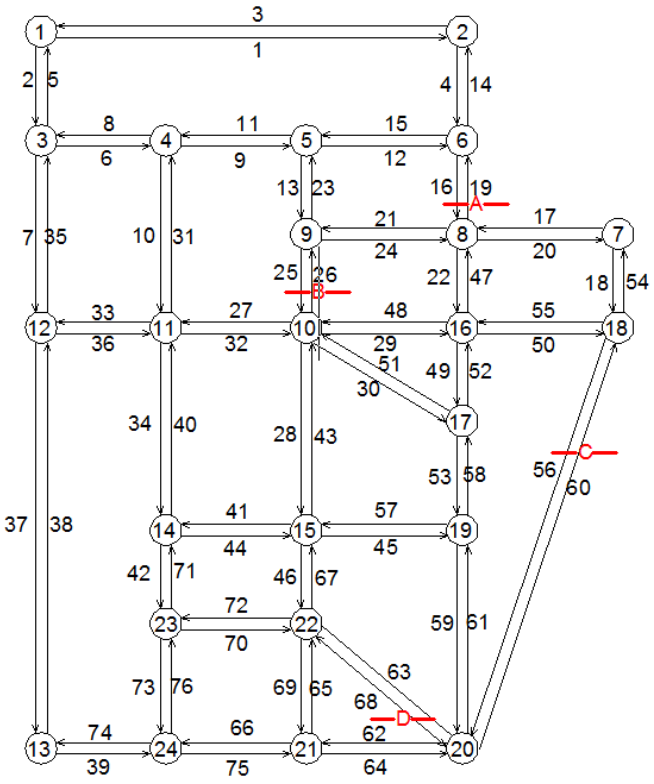

Figure 2.2 Sioux Falls Network

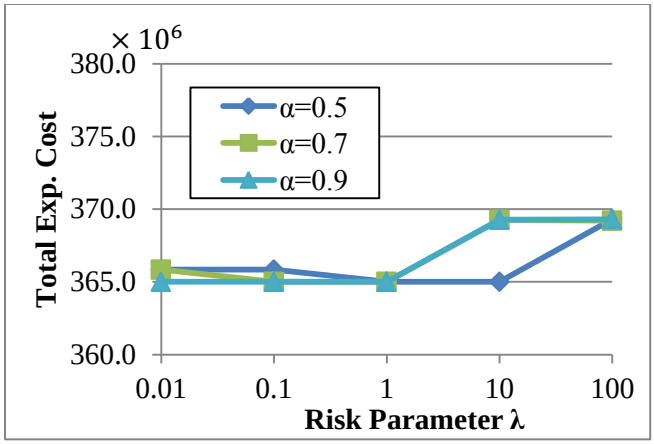

(a) CVaR

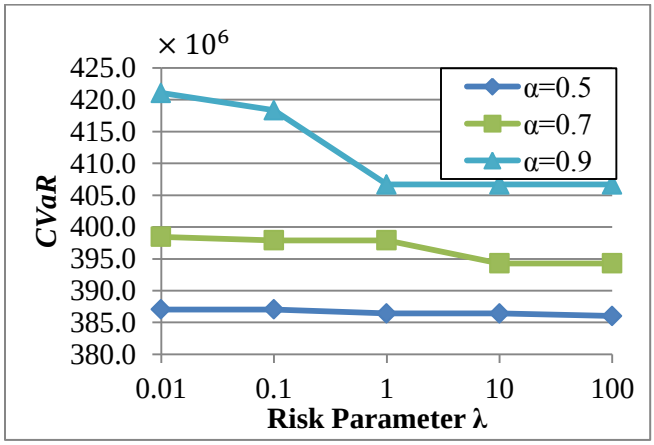

(b) Total exp. Cost

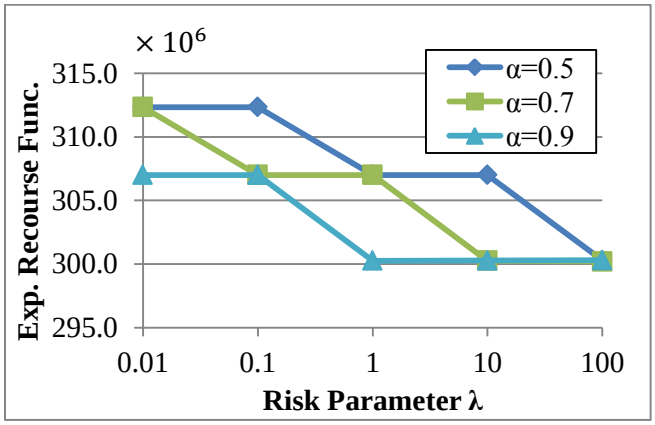

(c) Retrofit cost

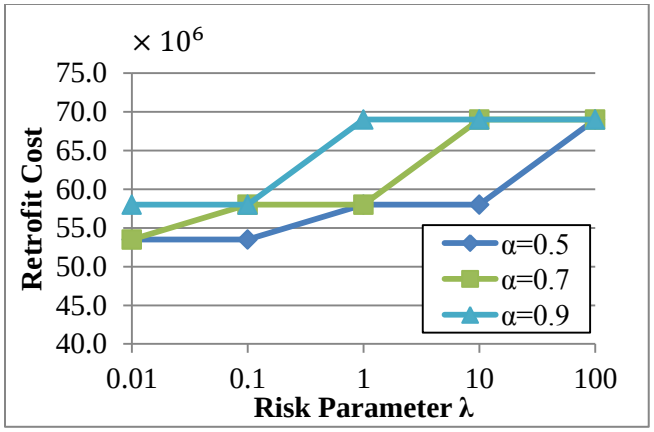

(d) Exp. Travel cost

Figure 2.3 Model results under different combinations of risk parameters

We first investigate the effects of risk parameters (i.e., α and λ) on model results and computational performances by running 15 combinations of three α (i.e., α =0.5, 0.7, and 0.9) and five λ (i.e., α = 0.01, 0.1, 1, 10, and 100) for 20 scenarios with $\bar{y} = 1500$. The confidence level parameter α controls the set of scenarios to be considered while the coefficient λ weighs the CVaR in the integrated mean-risk stochastic model. A higher α results in more scenarios to be considered and a higher λ will increase the weight of the CVaR. Through the numerical experiments, we intend to explore a best possible combination of the risk parameters and more importantly highlight the modeling insights through these numerical experiments on the integration of the risk measure (i.e., CVaR) into a two-stage stochastic programming framework. The main insight is to investigate whether a mean-risk model provides different solutions than a two-stage stochastic model. The breakdown of the total cost is plotted in Figure 2.3. The total mean-risk cost (or

objective value) is the summed total expected costs and weighted CVaR. The total expected cost is comprised of retrofit cost and the expected travel cost.

We will discuss the impacts of the risk parameters on the cost effectiveness and CVaR separately. Note that the specified α level represents the risk preference, which quantifies the mean value of the worst $(1 - \alpha)\%$ of the total costs. Figure 3a shows that when α increases the corresponding value-at-risk η account for the risk of larger scenario realizations. Thereby, larger α values would result in more conservative policies, which give more weight to worse scenarios. Also increasing the value of λ would leverage the weight and increase the relative importance of the risk term in the objective and thus would also lead to more risk-averse policies. Therefore, increasing the parameters α and λ implies a higher level of risk aversion. CVaR increases as α increases by the definition, i.e., a larger value of α accounts for larger realizations of the total cost. However, CVaR decreases as λ increases due to the changing trade-off between the expectation and the CVaR criterion. The total expected cost shown in Figure 2.3b is comprised of the retrofit cost in Figure 2.3c and the expected travel cost in Figure 2.3d. According to the results, increasing λ and α leads to more risk-averse policy with higher retrofit cost (i.e., enhanced retrofit strategies) and lower expected travel cost (implying reduced post-disaster capacity loss) in general.

We can also draw important managerial insights from the results. First, we can identify best possible parameters that can lead to balanced cost-risk solutions by the mean-risk model. For example, from Figure 2.3a and 2.3b, we found that when $\alpha = 0.5$

and $\lambda = 1$, both the total expected cost and the CVaR are at the lowest. This parameter setting among all tested combinations leads to a policy that best balance the cost and risk. Second, it is important to investigate if the mean-risk model provides different solutions from the traditional two-stage SP model. For this purpose, we also compare results by the mean-risk model with the two-stage SP model in Table 2.2, in which the results of the mean-risk SP model are based on the best risk parameter ($\alpha = 0.5$ and $\lambda = 1$). In the table, the CVaR value by the two-stage SP model was evaluated with given first-stage solutions and retrofit strategies for different bridges are labeled with strategy indexes. The inclusion of a risk term makes the solution more risk-averse, which is indicated by the difference in retrofit strategies for Bridge D. The mean-risk model adopts a more enhanced strategy than the two-stage SP model. As a result, the retrofit cost is higher, but the expected travel cost is lower, which also leads to an overall decreased total expected cost.

Table 2.3 Comparisons between Two-Stage SP and Mean-Risk SP

	Two-Stage SP	$\alpha = 0.5, \lambda = 1$
CVaR	398.6	386.4
Total Exp. Cost	367.9	365
Retrofit Cost	49	58
Exp. Travel cost	318.9	307
Bridge A Strategy	3	3
Bridge B Strategy	3	3
Bridge C Strategy	2	2
Bridge D Strategy	0	2

In Table 2.4, we present optimality gap, CPU times, and number of iterations for the different combinations of risk parameters, i.e., three α =0.5, 0.7, and 0.9 and five λ = 0.01, 0.1, 1, 10, and 100 for 20 scenarios with $\overline{y} = 1500$. The two-stage SP model solution performance is also included for comparisons, which is essentially $\lambda = 0$ and tolerance gap ϵ = 1%. We found that for all combinations of risk parameter values, the problems can be solved to optimal within 1% gap. Also, CPU times and the number of iterations used are similar across all cases. For the same number of iterations, ends up with different computing times, which implies that sub-problem complexity depends on the combinations of risk parameters. For a smaller tolerance, we expect improved solutions but more iterations and longer computing times.

Table 2.4 Solution performance with 20 scenarios

		Optimality gap	CPU time (min)	# of iterations
Two-stage SP ($\lambda = 0$)		0.96%	116.3	28
	$\alpha = 0.5$	0.71%	98.0	24
$\lambda = 0.01$	$\alpha = 0.7$	0.71%	95.4	24
	$\alpha = 0.9$	0.00%	110.5	27
	$\alpha = 0.5$	0.71%	100.0	25
$\lambda = 0.1$	$\alpha = 0.7$	0.00%	114.8	28
	$\alpha = 0.9$	0.84%	88.5	21
	$\alpha = 0.5$	0.00%	105.9	26
$\lambda = 1$	$\alpha = 0.7$	0.12%	113.8	28
	$\alpha = 0.9$	0.25%	73.2	18
	$\alpha = 0.5$	0.89%	99.4	23
$\lambda = 10$	$\alpha = 0.7$	0.00%	110.5	27
	$\alpha = 0.9$	0.00%	88.9	20
	$\alpha = 0.5$	0.73%	104.0	24
$\lambda = 100$	$\alpha = 0.7$	0.00%	110.8	27
	$\alpha = 0.9$	0.00%	85.3	20

Table 2.5 Costs and solution performance for different numbers of scenarios (|K|)

# of Scenarios	10	20	50	100
Obj. Value (10^6)	705.41	762.92	781.54	781.87
CVaR (10^6)	360.71	397.91	410.28	407.86
Total Exp. Cost (10^6)	344.70	365.01	371.26	374.01
Retrofit Cost (10^6)	58.00	58.00	71.50	87.00
Exp. Recourse func. (10^6)	286.70	307.01	299.76	287.01
Optimality Gap	0.03%	0.95%	0.85%	0.44%
CPU Time (min)	33.20	94.82	215.05	405.30
# of Iteration	18	23	25	23

We also investigate the impacts of the different sized scenario sets (i.e., $|K| = 10,20,50,100$) on the system costs and solution performances while other model parameters remain unchanged, i.e., the same four bridges, $\lambda = 1$, and $\alpha = 0.7$. The number of low, median and high risk scenarios also has a ratio of 5:3:2. We randomly generate scenarios as follows: (1) in all sets, the numbers of low-, median-, high- risk scenarios are in the ratio 5:3:2; and (2) the probabilities of scenario occurrences are uniformly distributed in each set. We report the model results and solution performance in Table 4. With a larger set of scenarios, the CVaR and the total expected costs are generally higher as essentially larger realizations are accounted. This is also implied by the increased retrofit cost. However, the expected travel cost can increase or decrease, partially because of the varied optimality gaps. The computing times increase with the number of scenarios. This is because the computing time for solving one iteration is in

general proportional to the number of scenarios. Although the numbers of iterations are relative steady across different number of scenarios as observed, it takes longer to solve one scenario with more scenarios.

6. Conclusions and future work

We develop a mean-risk MINLP for transportation network protection (e.g., retrofitting highway bridges) hedging against extreme disasters (e.g., earthquakes) on a system level, where *CVaR* is considered as the risk measurement and integrated into the single optimization framework. This is the first study that explicitly considers *CVaR* as the risk measure in the field of transportation network protection. The mean-risk formulation is not obviously a convex optimization problem. By reformulating of the problem, we show that the recourse function is convex in the bridge retrofit variables. We develop a decomposition algorithm based on GBD to solve the large-scale MINLP.

This study demonstrates the applicability of the model and decomposition method using two numerical examples, a small nine-node network and the well-known Sioux Falls network. The nine-node network is used to justify the solution quality of the proposed decomposition method by comparing their performances with the exact solutions that are obtained from using the commercial solver BONMIN. The Sioux Falls network example demonstrates that the proposed solution method makes the model applicable for large-scale problems. We explore the correlations between risk parameters and retrofit decisions using the Sioux Falls network. We found that the retrofit strategies

are responsive to the risk parameters and scenario set. The computing time for large instance is proportional to the number of scenarios of the instance.

Several future directions would be worth research efforts, which involve both the modeling and algorithmic development. From modeling perspective, the traffic equilibrium may be a more realistic assumption to model route choices of network users. The integration of equilibrium will make the model a Mathematical Program with Equilibrium Constraints (MPEC), which is notoriously difficult to solve. Second, more algorithmic development (including heuristics) may be worth further exploration to prepare the model for real-world scale networks.

Chapter 3 A Bi-level Framework for Efficient Allocation of Resources for Bridge Retrofit

1. Introduction

According to the American Society of Civil Engineers 2013 Report Card (ASCE, 2013), one in nine of the bridges in the U.S. are structurally deficient and vulnerable to extreme events. Many states are facing the challenge of extending the remaining life of existing bridges through retrofit programs with limited funding resources. Since it is neither practical nor possible to retrofit all the bridges to their full performance, it is important to effectively allocate resources to the bridges that are not only the most in need of repair but also have significant impacts on the transportation network. Conventional engineering practice prioritizes at-risk bridges primarily based on structural assessment and neglects the impacts of bridges on transportation network (Chandrashekaran & Banerjee, 2014; Wang, et al., 2010). On the other hand, research in bridge network protection often simplifies the relationship between the bridge's traffic capacity and the retrofit cost as linear functions (Liang Chang, et al., 2012; C. Liu, et al., 2009). That is, the more funds spent, the higher bridge traffic capacity will be. We propose a new approach to integrate traffic network modeling and individual structure enhancement into a bi-level optimization framework and the goal is to minimize the retrofit costs and travel delay in the face of extreme events.

In this study, both network modeling and structural assessment are integrated into a bi-level modeling framework, in which the upper-level model determines the optimal allocations of retrofit resources to bridges while the lower-level model explicitly calibrates the traffic capacity-cost relationship using finite element (FE) models for each individual bridge.

The upper level is a network optimization problem used to minimize the bridge retrofit cost and traffic delays. Uncertainty is inevitable in making bridge retrofit decisions in the face of extreme events. We develop a mean-risk two-stage stochastic programming framework (Lu, et al., 2015) to tackle the uncertainty, in which the uncertainty space is approximated by a set of discrete scenarios and the concept of Conditional Value-at-Risk (CVaR) (Rockafellar & Uryasev, 2000) is adopted to reduce the probability of a retrofit strategy that incurs large losses. This method also extends the capability of handling uncertainty in the traditional two-stage stochastic programming method (i.e., expectation of outcomes of scenarios) by allowing for flexible risk preferences (i.e., user-specified reliability levels).

The lower level of the framework determines the optimal retrofit alternatives for a RC bridge pier to remain serviceable level of shear strength at different funding levels. General speaking, RC bridges should avoid brittle failure mode against an extreme earthquake event. A satisfactory seismic response for RC bridge is obtained by developing ductile inelastic flexural hinging at their plastic hinges. However, locating such plastic hinges in bridge superstructures is difficult and it is not desirable (Priestley, et al., 1994). Therefore bridge piers become major sources for bridge structural ductility

and energy dissipation. As a function of ductility, the shear strength of piers should remain certain level defined by capacity design to avoid brittle shear failure.

In this chapter, the shear strength of the intentional cracked piers and the damaged piers with steel jacket are investigated by using software ANSYS 14.5. A set of models with different retrofit parameters is evaluated through the comparison of healthy and unrepaired models. The retrofit parameters in this study contains the height and width of steel plates used for bridge pier retrofit. We assume that the retrofit cost for a pier can be determined by the weight of the material used and number of labor hours for applying the retrofit. This study defines the improvement in shear strength as a nonlinear function of available funding, then translates the bridge pier shear strength into traffic carrying capacity and feed this information into the bi-level modeling framework. In particular, we apply robust design principles to investigate the possible trade-off relationships between bridge pier performance using different retrofit strategies and the cost of retrofit under the threats of uncertain natural disasters. This nonlinear relationship can be reflected by Pareto frontier of retrofit design, a collection of optimal retrofit designs that are superior to all other retrofit alternatives. The objective of the lower-level optimization problem is to ensure that dominated designs, which would indicate inefficient use of resources, are avoided. Therefore, the objective of the lower-level optimization problem is to find the set of optimal retrofit alternatives considering cost and resilience that forms a Pareto frontier for each earthquake scenario.

This chapter is organized as follows. In Section 2, a review of relevant literature details the network protection problem as well as bridge structural enhancement problem.

In Section 3, the bi-level modeling framework is discussed in details, followed by a numerical study based on the benchmark Sioux Falls network in Section 4. Finally, the remarks and future research are briefly summarized in Section 5.

2. Literature review

Prior studies on bridge protections can be generally grouped into two major categories - transportation network protection problems and structural enhancement problems. The first category of studies focuses on the long-term impact of bridges on traffic network performance while the second category focuses on retrofit strategies on the enhancement of individual structure.

Transportation network protection problem is essentially a network design problem, which has been the subject of many extensive studies over the past few decades (LeBlanc, 1975; Luathep, et al., 2011; Magnanti & Wong, 1984; Yang & H. Bell, 1998). Most prior research efforts were based on the assumption that bridge damage is either fixed for a specific event (Fan, et al., 2010; Y. Huang, et al., 2014; C. Liu, et al., 2009), or that the bridge performance has multiple possible states after a disaster (Liang Chang, et al., 2012; Golroo, et al., 2010; Kim, et al., 2008; Peeta, et al., 2010). In the former category, C. Liu, et al. (2009) and Fan, et al. (2010) formulated a stochastic programming model to minimize the post-disaster network traffic delay and associated risk. Similarly, Y. Huang, et al. (2014) developed a retrofit decision scheme where the costs of retrofit strategies are certain percentage of new construction costs. In the latter category, discrete damage states

that were known a priori or established through the use of fragility curves have been used to evaluate structural performance of bridges. For instance, Golroo, et al. (2010) detailed a resource allocation optimization problem based on the reliability of the transportation infrastructure. Peeta, et al. (2010) developed a two-stage problem to maximize the post-disaster connectivity that was based on the known link failure probability, and Kim, et al. (2008) evaluated the impact of an earthquake on road networks using fragility curves and static traffic assignment method. Finally, in a recent study, Liang Chang, et al. (2012) maximized network post-disaster evacuation capacities by using established bridge fragility curves to determine the damage state of each bridge, then convert them to bridge post-earthquake traffic capacities.

For structural enhancement problem, studies focused on this category primarily involved using the FE analysis to determine the structural performance and effectivities of retrofit strategies. For example, in their study of Reinforced Concrete (RC) bridge piers, Z. Sun, et al. (2008) used a set of experiments on scaled pier specimens to compare against simulation models to evaluate the capacity of FE analysis software to model the hysteric behavior of RC piers. J. Zhang, et al. (2011) and Xu and Zhang (2011) used the shear-flexure interactive behavior of RC bridge piers as structural performance in their developed hysteretic models and implemented the models by using FE analysis. In another experiment, Lampropoulos and Dritsos (2011) performed FE analysis to examine the behavior of RC jacket strengthened columns under monotonic and cyclic loading. Chandrashekaran and Banerjee (2014) studied multiple retrofit strategies in terms of the

thickness of the column jackets for a multi-span bridge where the structural performance is evaluated by FE analysis.

We integrate the transportation network protection and structural enhancement problems into a bi-level modeling framework. Structural enhancement problem involves the investigation of the relationship between retrofit levels and the structural performances of bridges, which must be obtained through a rigorous yet realistic analysis. On the other hand, transportation network protection problem requires traffic capacity-retrofit cost relationship, which can be converted from relationship between structural performances and retrofit levels. To seamlessly integrate the two problems, we must find a way to bridge the two relationships in our integrated framework.

3. Bi-level resource allocation modeling framework

The proposed resource allocation modeling framework at the upper level is demonstrated using a well-known example of the Sioux Falls network shown in Figure 3.1 (LeBlanc, et al., 1975) with 24 nodes and 76 directional links. Let us assume that there are four bridges, labeled as A to D in the network, each of which occupies both directions of traffic links and is subject to potential disasters.

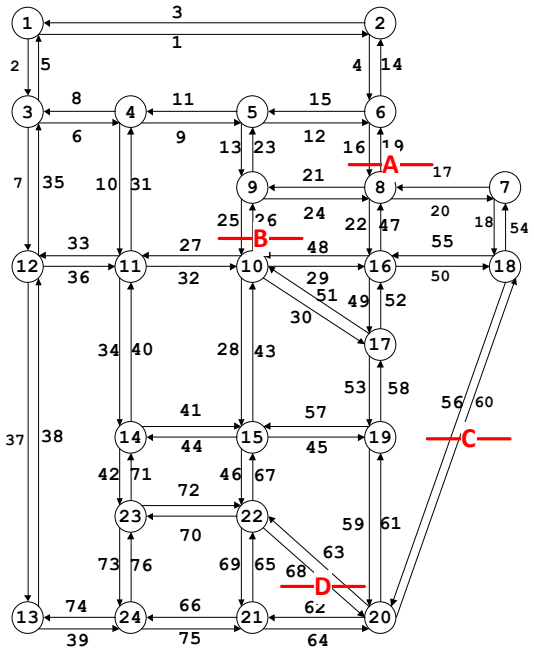

Figure 3.1 Sioux Falls network

The four bridges in the network are not independent of each other. For instance, the failure of bridge C would detour the traffic from node #20 to #18, which was originally traversed through link #60 to a longer path –of links #61, 58, 52 and 50. As a result, the network travel cost may increase due to the detours and resulting congestion caused by the redistributed traffic. Thus, at-risk bridges must be retrofitted to avoid undesirable consequences to the network. The conventional engineering practice of prioritizing bridges primarily based on the structural deficiency, may not guarantee system optimality from the perspective of network traffic operations. For instance, consider that i) bridge D is in a worse structural condition than bridge C and ii) that there are insufficient funds for retrofitting both bridges C and D. According to prioritization based on structural

deficiency, bridge D will be the preferred choice for retrofit, leaving bridge C with a higher chance of failure in extreme events. This solution is suboptimal, as the failure of bridge D would affect fewer links than the failure of bridge C. Thus, from a traffic management perspective, bridge C is more important to the network. Consequently, a tradeoff must be made between the impacts on traffic network and the need for structural enhancement. However, it is impossible to determine which bridge must to be rehabilitated until one solves the network optimization problem, which requires knowledge (e.g. trade-off relationship between structural performance and retrofit level) from the structural level. Through this proposed bi-level modeling framework, it will be possible to couple the system-level resource allocation at the upper-level with the individual bridge structural performance by the use of FE analysis at the lower level.

The uncertainties of disruption on different bridges caused by natural or man-made disasters further amplify the difficulty. First, the modeling of the uncertain occurrence of disruptions to the network needs to integrate the design of the infrastructure rehabilitation scheme. Second, at the upper level, uncertainties related to the occurrence of different disruptions on different bridges are normally approximated by a set of discrete scenarios and must be determined through a stochastic modeling framework (e.g., stochastic programming(Birge & Louveaux, 2011) and robust optimization(Kouvelis & Yu, 2013)), resulting in risk-neutral or overly conservative solutions. This proposed risk integrated stochastic modeling framework offers greater modeling flexibility that can lead to a spectrum of risk adverse solutions.

In this study, we created a novel methodology to establish infrastructure retrofit strategies that operate under uncertainty. The proposed modeling framework integrates the retrofit of individual infrastructure with resource allocations to minimize the retrofit and travel costs for the entire network. Figure 3.2 depicts the bi-level modeling framework for the Sioux Falls transportation network.

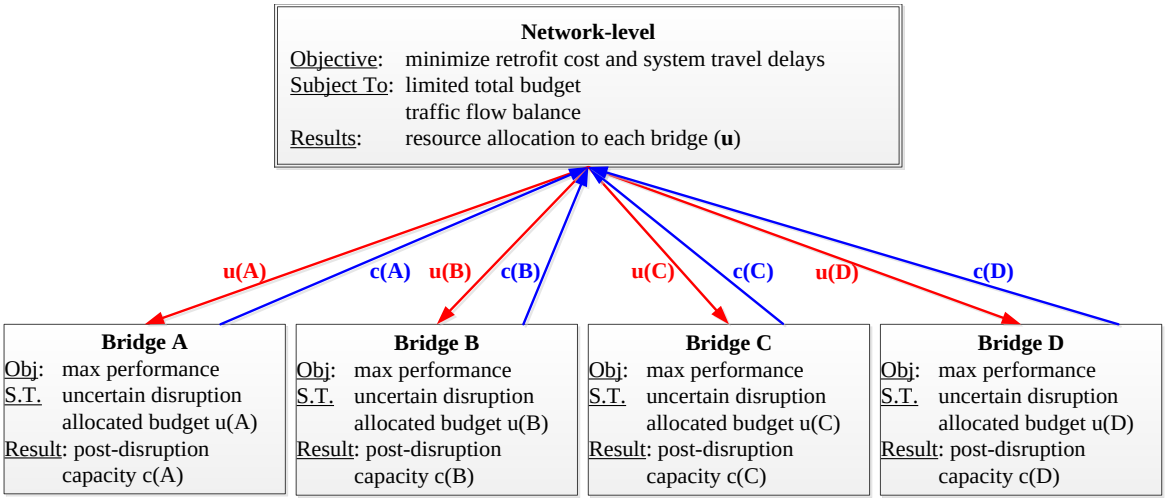

Figure 3.2 Bi-level framework for bridge retrofit

At the upper level, resource allocation (denoted as u) is made based on a network optimization problem with an objective to minimize the retrofit and travel costs given a fixed amount of available resources. Because individual links within a network are interdependent in the way they support the traffic flow, traffic assigned to each bridge is dependent on the availability and capacity of the other bridges in the network. This

interdependency is captured by network optimization model at the upper level, which determines the resource that each bridge receives (indicated by the red arrows in Figure 3.2). At the lower level, the framework determines the traffic capacity of each bridge under the allocated budget. The resulting performance index of each bridge (denoted as c) in terms of traffic capacity, then feeds back to the network level model (indicated by the blue arrows in Figure 3.2). In general, a higher budget allows for a more extensive retrofit strategy, which results in a more functional structure; In order to get a closed form mathematical relationship between the retrofit level and structural performance, we use the FE analysis to simulate the levels of retrofit strategy and correspondent structural performance. We then obtain the relationship between traffic capacity of bridge and cost by using second order least square regression of multiple simulation results.

In the following subsection, we will first separately discuss the upper and lower levels of the problems in sections 3.1 and 3.2, respectively, followed by the discussions of solutions to this bi-level problem in section 3.3.

3.1 Upper-level sub-problem: retrofit resource allocation over network

At network level, we adopted a mean-risk formulation (Lu, et al., 2015) with the assumption that traffic flow can be controlled to achieve "system optimal" condition. The focus herein is the integration of structural assessment and network modeling. Let $G(N, A)$ denotes the transportation network, where N is a set of nodes and A is a set of links. Next, R and S ($R \subseteq N, S \subseteq N$) denote the sets of origins and destinations on the

network. Finally, $\overline{A}$ ($\overline{A} \subset A$) denotes the set of links that are subject to disruptions, where $\left|\overline{A}\right| = \overline{m},$. If bridge a ($a \in \overline{A}$) is retrofitted by strategy h, ($h \in H$), the binary decision variable $u_a^h = 1$; otherwise, $u_a^h = 0$. For an origin-destination (O-D) pair (r, s), $x^{rs} \in \mathbb{R}_+^m$ is the link flow vector and $q^{rs} \in \mathbb{R}_+^n$ is the vector of travel demand between an O-D pair. The total flow on link a is v_a. Unsatisfied travel demand, due to various reasons, is captured by decision variable d^{rs} in the model with an imposed penalty cost in the objective function.

Scenarios, defined as the combination of different disruptions to bridges in the network, are combined with a set of occurrence probability estimates. Let k describe a scenario with corresponding probability p^k. Let K denote a set of random events, $k \in K$. We assume that the selected retrofit decision variable $u_a^h = 1$ will affect the post-disruption bridge capacity $\hat{c}_a^k$; that is $\hat{c}_a = c_a \sum_{h \in H} u_a^h \theta_a^{h,k}$, where c_a is the bridge traffic capacity before disruption, and $\theta_a^{h,k}$ is a parameter describing the post-disruption link capacity ratio. The retrofit strategies are mutually exclusive for an at-risk bridge, including do-nothing option. Therefore, $\sum_{h \in H} u_a^h = 1, \ \forall a \in \overline{A}$.

$$\min_{u \in U} (1 + \lambda) c^T u + E(Q^k(u)) + \lambda(\eta + \frac{1}{1-\alpha} E([Q^k(u) - \eta]^+)) \tag{3-1}$$

$$s.t. \qquad c^T u \leq B \tag{3-2}$$

$$\sum_{h \in H} u_a^h = 1, \ \forall a \in \bar{A}, \tag{3-3}$$

$u \in \{0,1\}^m, \eta \in \mathbb{R}$.

$$Q^k(u) := \min_{v,x,d} \gamma[v^T t] + M \sum_{r\in R, s\in S} d^{rs,k} \quad (3\text{-}4)$$

$$Wx^{rs,k} = q^{rs} - d^{rs,k}, \ \ \forall r \in R, s \in S, k \in K, \quad (3\text{-}5)$$

$$v_a^k = \sum_{r\in R} \sum_{s\in S} x_a^{rs,k}, \ \ \forall a \in A, k \in K, \quad (3\text{-}6)$$

$$t(u, v_a) = t_0 \left[1 + \beta \left(\frac{v_a}{\hat{c}_a^k}\right)^4\right], \ \ \forall a \in A, \quad (3\text{-}7)$$

with $$\hat{c}_a^k = \begin{cases} \sum_{h\in H} u_a^h \theta_a^{h,k} c_a, \forall a \in \bar{A} \\ c_a, \forall a \in A \backslash \bar{A} \end{cases}, \forall k \in K,$$

where η is the value-at-risk, $\eta \in \mathbb{R}$, and $[z]^+ = \max\{0, z\}, \forall z \in \mathbb{R}$.

The objective (3-1) is to minimize the total expected system cost and the corresponding monetary value of risk. Here $f^k(u) = c^T u + Q^k(u)$ is the total cost function for scenario k, consisting of first stage cost $c^T u$ and recourse function $Q^k(u)$. The recourse function encompasses the travel cost and the penalty cost of unsatisfied demand $d^{rs,k}$. Constraint (3-2) is the budget constraint, c is the cost vector for all bridges and retrofit alternatives and B is the total retrofit budget. Constraints (3-3) ensure that each bridge receives only one retrofit strategy. The recourse function is defined in equation (3-4), in which v is a vector of link flow v_a^k for link a scenario k, γ is a parameter that converts travel time to money value, and M is the penalty for the unsatisfied demand $d^{rs,k}$. Constraint set (3-5) assures that travel demand is either satisfied

or penalized, where W is a node-link adjacency matrix. Constraints (3-6) describe the relationship between the total link flow v_a^k and link flow $x_a^{rs,k}$ for each O-D pair rs. The equation set (3-7) describes the travel cost function - the Bureau of Public Roads (BPR) function. The travel time relates to link flow v and post-disruption link capacity.

3.2 Lower-level subproblem: development of structural performance-retrofit level trade-off charts

The lower-level problem is to derive a relationship between retrofit cost and bridge's traffic capacity through determining a retrofit level and structural performance relationship. The relationships between the four components are interconnected and described in Figure 3.3.

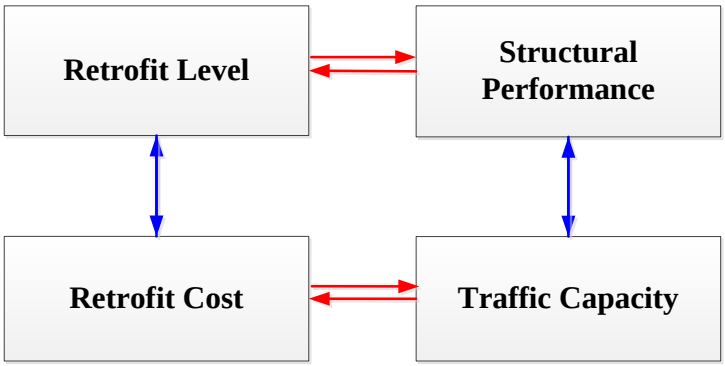

Figure 3.3 The connections between retrofit level, retrofit cost, structural performance and traffic capacity

There are several steps to derive the relationship between bridge's traffic capacity and cost. First, we need to decide alternative retrofit strategies and calculate the correspond costs, which normally are different. Then, we use nonlinear finite element (FE) models to simulate the improved structural performance of the bridge that correspond to the different retrofit strategies.

Note that computationally evaluating structural performance given retrofit strategies is a generic process, which can be applied to any bridge or bridge component. One aspect that needs attention is the simulation of bridge damages due to disruptions. The disruption can be in any form, which varies from a simplified pushover to seismic loading. Another important aspect is the indicator for structural performance. In our case study, we use shear strength for example. However, one can focus on many other aspects of the bridges and use other indicators for the structural performance.

The next step is to connect structural performance to traffic capacity. We associate the structural performance to traffic capacity proportionally. There are some restrictions on the value of variables for traffic capacity and structural performance to make them more close to reality. We set a minimum traffic capacity for the bridge link and a maximum traffic capacity after disruption which is the original traffic capacity of the bridge link. Also, there is a maximum allowable structural performance improvement, beyond which the improved structural performance has no further impact on link traffic capacity.

Finally, we can evaluate relationship between the traffic capacity and retrofit cost and use the relationship as an input for upper level framework.

3.3 Solution to the bi-level resource allocation model

The challenges include establishing connections between the sub-problems at two levels in the solution process and equilibrium when the overall system cost is minimized. Both sub-problems should be solved simultaneously and often requires converting the bi-level problem to a single-level problem, which is computationally challenging. We instead propose a bottom-up solution. In particular, the lower-level sub-problem yields a nonlinear relationship between bridge's traffic capacity and cost. For each retrofit level, the use of FE method will result in the correspondent performance of the structure. We convert the structural performance-retrofit level relationship to bridge traffic capacity-cost relationship. Each bridge has a correspondent nonlinear relationship between traffic capacity and cost, which is used in the upper-level network problem as model input. This large-scale combinatorial optimization problem is decomposed into a master and sub-problems where first stage integer variables are temporally fixed, which renders the remaining problem tractable. Lagrangian duality is then used to generate cuts for the master problem.

4. Numerical examples

Numerical experiments are then used to demonstrate this bi-modeling framework. The structural assessment at the lower level is discussed and illustrated by a bridge pier example. The nonlinear trade-off traffic capacity-cost assumptions are then used in the upper-level network sub-problem for structural assessment.

4.1 Pier structural assessment for lower level model

In our case study, the disruptions due to natural or man-made disaster happened to the bridge pier takes the most simplified form. In particular, we apply lateral loads at the top of the bridge piers, which have fixed supports at the bottom to simulate the shear failure mode. We assume that all bridges in the network are two-span bridges with a single middle pier. Therefore, the pier, which is the critical part of the bridge, should retain a certain level of shear strength, a specification of structural performance, to avoid brittle shear failure mode during natural disasters. The structural assessment simulates bridge piers with cracks, where steel jacketing was selected as retrofit alternatives that represent different retrofit levels. Concrete, with nonlinear material properties, and steel, with bilinear material properties, are used in the construction of RC bridge piers. To model the current condition of the bridges, we assume that there is a horizontal crack in each of the bridge pier in the FE model. In this study, we specifically refer retrofit alternatives to the steel plates with different thickness. The steel plates are large enough to cover the initial crack and are partly glued to the pier to avoid over retrofit. The nonlinear material

properties of RC and the intentional cracks makes a convergence of FE analysis difficult. We use finer meshing around the cracks and use proper convergence criteria to mitigate that difficulty. Finally, we use the least square regression method to form a nonlinear curve that best approximate the nonlinear relationship between improved shear strength and steel plate thickness.

Specimen geometry

We developed a scaled version of typical RC bridge piers model using the ANSYS FE analysis software (ANSYS). The cross section of the pier was rectangular with dimension of $300\ mm \times 400\ mm$, and a height of $900\ mm$. The longitudinal reinforcement ratio of the pier was set at 2% of the gross cross-section area, and the transverse reinforcement ratios for the plastic hinge region and other region were 1% and 0.5%, respectively. The positon of the plastic hinge region was assumed somewhere within the bottom $300\ m$ of the pier.

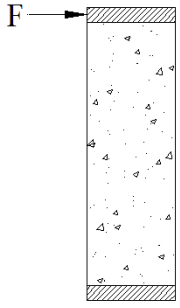

Figure 3.4 Schematic view of bridge pier

Model description

The specimen is modeled using the SOLID65 concrete element that is capable of crushing in compression and cracking in tension. The top slice under the load and the bottom slice near the support of the pier are modeled as SOLID45 elements to avoid cracking at early stage.

Normally shear transfer coefficients range from 0.0 to 1.0, where 0 represents a smooth crack (no shear transfer exists) while 1.0 represents a rough crack (complete shear transfer). There would be convergence problem if the shear transfer coefficients are set to a small value. In this study, the shear transfer coefficient β_t for open crack is assumed to be 0.6, while for closed cracks, the shear transfer coefficient β_c is assumed to be 1.0.

The concrete and steel plate material properties are shown in table 3.1. The SOLID65 element has a smeared rebar option in which the orientation of rebar is defined by three angles. The material properties for rebar are also shown in table 3.1.

Table 3.1 Material properties

Material number	Material properties	Value
1	Concrete	
	Multi-linear isotropic	
	Modulus of Elasticity	15276 MPa
	Poisson's ratio (PRXY)	0.2
	Compressive Strength	19 MPa
	Tensile Strength	2.22 MPa
	shear transfer coefficient for open crack	0.6
	shear transfer coefficient for closed crack	1
2	Steel plate and rebar	
	Bilinear isotropic	
	Modulus of Elasticity	200000 MPa
	Poisson's ratio (PRXY)	0.3
	Yield Strength	420 MPa

Using SOLID65 element to define concrete requires obtaining multi-linear isotropic material properties to properly model the concrete material. The concrete material properties are based on the equation of complete curve for compressive-strain of the concrete (Guo, 2014), where dimensionless coordinates $x = \frac{\varepsilon}{\varepsilon_p}$ and $y = \frac{\sigma}{f_c}$ are used to describe the curve mathematically. This description is expressed as

$$y = ax + (3 - 2a)x^2 + (a - 2)x^3, \ x \leq 1 \qquad (3\text{-}8)$$

where $a = \frac{E_0}{E_p}$ and $1.5 \leq a \leq 3.0$. Equation (1) shows the ascending branch ($x \leq 1$) of the equation and set $a = 1.7$ here. We assume that there is no descending branch in our model, that is, when $x \geq 1$, $y = 1$.

The uniaxial stress-strain curve is shown in Figure 3.5.

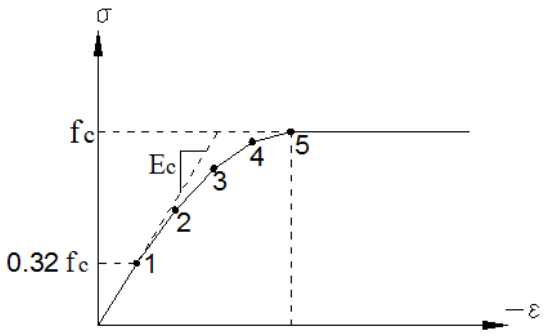

Figure 3.5. Constitutive relations for concrete.

A bi-linear stress-strain relationship is used for steel material. The stress-strain curve is shown in Figure 3.6.

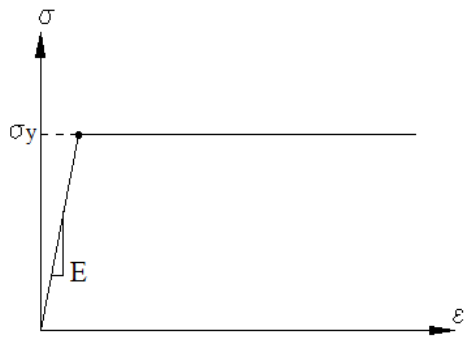

Figure 3.6 Constitutive relations for steel.

Finite element model development

There are several assumptions that associated with SOLID65 concrete elements. One assumption is the base will be fixed and all base nodes are restrained in three directions to model a rigid foundation for bridge pier. We apply a displacement controlled lateral load on the topside of steel plate placed on the top of the pier to obtain ultimate shear strength.

To model the current condition of a damaged pier, we assume the pier has an initial crack that is horizontal. The initial horizontal crack with different width, length and location is generated in the FE model to simulate different damage conditions.

Also steel plates with different length and thickness are modeled to cover the initial crack as a strengthening material. We assume that only parts of the steel plate are glued

to the specimen, which is, the upmost potion and bottommost potion of the steel plate are glued to bridge pier.

Figure 3.7 show models' geometry with and without jacketing. There is a 50 mm thick steel plate above the specimen and a 50 mm thick steel plate below the base. A hexahedral meshing is used for the RC bridge column with side length of 50 mm. Plastic hinge region as well as the steel plate jacket are meshed by using elements with 25 mm length.

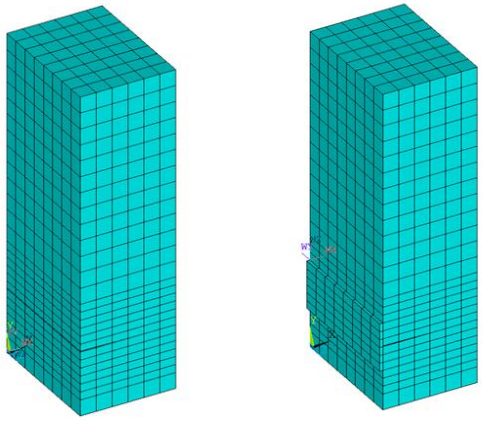

Figure 3.7 Models for damaged piers with and without 10 mm steel plate jacketing.

The boundary conditions are set to simulate experiment conditions. The base area is restrained in three directions while the load is applied on the top area of steel plate. A total 24 mm displacement in x direction is applied on the top area.

Nonlinear trade-off for structural performance-cost

To obtain the strategies that both reduce the cost and improve the shear strength for piers, we tested models with different dimensions of the steel jacket. We assume that the thickness of the steel plates w ranges from 3 mm to 15 mm. We then record the resistant forces in x direction for all nodes locating in the bottom area, and then total the nodal resistant force to form a single resistant force F_x for the base. The resistant force at 24 mm displacement corresponds to the shear strength for the pier. Using the resistant force at the bottom and the corresponding displacement in the x direction at the top area of the pier, we can generate load-displacement diagrams for all specimens. The damaged pier without the steel plate jacketing is selected as the control group. The shear strength of damage pier without the retrofit is recorded as F_{x0}. Thus we can attain the shear strength improvement $\Delta F = F_x - F_{x0}$ for each specimen. Figure 3.8 shows the pushover results for non-retrofit pier and the representative retrofit alternatives.

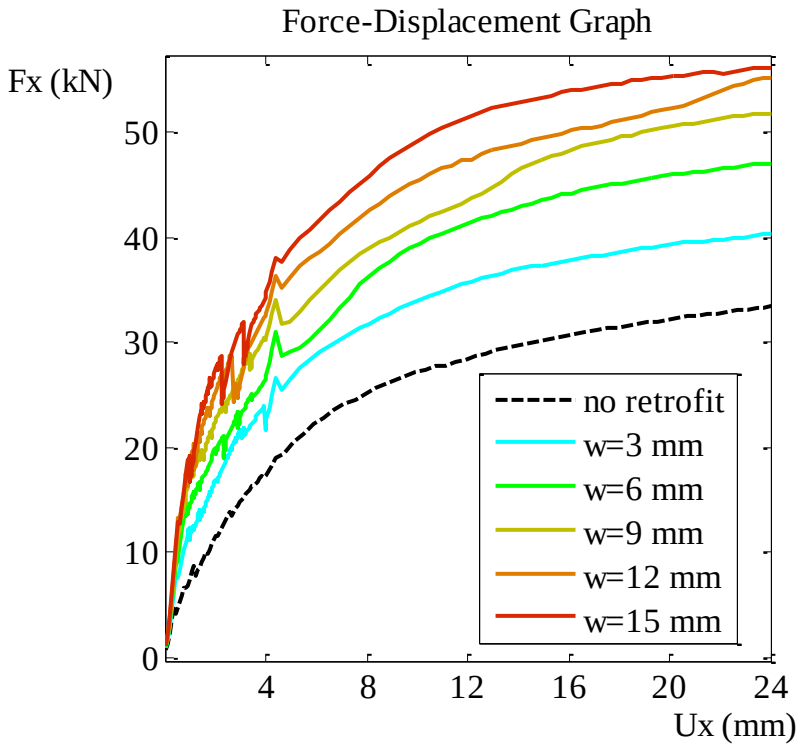

Figure 3.8. Load-displacement diagrams for model with different thickness of steel plate jacketing

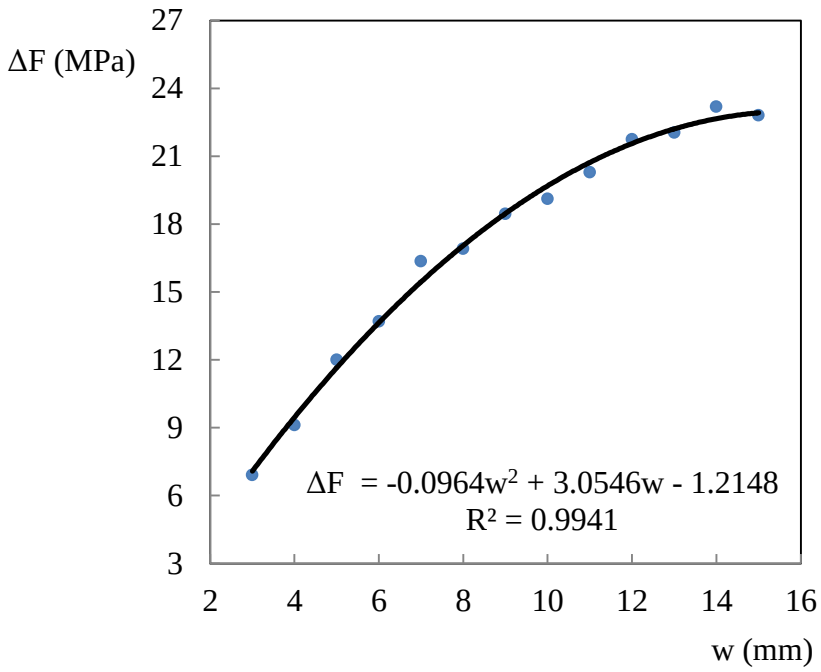

Figure 3.9. Shear strength improvements for different steel jacket thickness

We tested 13 different thickness of steel jacket. A second order least square regression is used for these 13 data points. The R squared value equals 0.9941 and sum of squares equals 1.9892 which shows the data fits very well for this second order statistic model. The regression function can then be used as the Pareto frontier function for this pier.

In Figure 3.9, gain in structural resilience (improved shear strength, y-axis) will result in a higher cost (thickness of steel jacket, x-axis). This trade-off relationship indicates that increasing the available project funding leads to a more resilient design. The structural resilience increases significant with the increase of steel plate thickness at the beginning, but beyond a certain point it becomes much less significant. Using robust

design principles will enable us to select the most efficient retrofit designs for a certain budget level. Once the Pareto front is obtained, given the available budget from the upper level, the lower level can use a 'lookup' table and indicate what would be the corresponding gain of shear strength and traffic carrying capacity.

4.2 Sioux Falls network analysis

In this section, we demonstrate the application of the bi-level model through the use of the Sioux Falls network shown in Figure 3.1. Based upon comparisons with linear traffic capacity-cost relationship that has been widely adopted in prior research studies and engineering practice, this integrated FE analysis in our proposed bi-level model can offer more cost-effective solutions.

Conversion of steel plate thickness to monetary cost: The lower-level problem yields the relationship between the shear strength improvement and steel plate thickness, which is converted to bridge's traffic capacity and cost relationship through a two-step process. The *first* step involves relating the retrofit cost to the steel plate thickness using equation (3-9):

$$rc_a = s_a(c_l + w * c_m) \tag{3-9}$$

where rc_a denotes the retrofit cost for bridge a, s_a denotes the size of bridge a, lc represents the unit labor cost, w is the steel plate thickness, and mc is the unit material cost. The retrofit strategies are denoted as "h0"-"h4", with corresponding steel jacket thicknesses of 0, 3 mm, 6 mm, 9 mm, 12 mm thickness of steel jacket (w), respectively.

The retrofit costs for different bridges under different strategies are provided in Table 3.2. Note that a bridge is represented by two directional links in this study.

Table 3.2 Retrofit cost ($1M) for all bridges

Bridges	Strategy				
	h0	h1	h2	h3	h4
link16	0.00	1.96	2.92	3.88	4.84
link19	0.00	1.96	2.92	3.88	4.84
link25	0.00	11.76	17.52	23.28	29.04
link26	0.00	11.76	17.52	23.28	29.04
link56	0.00	15.68	23.36	31.04	38.72
link60	0.00	15.68	23.36	31.04	38.72
link63	0.00	1.96	2.92	3.88	4.84
link68	0.00	1.96	2.92	3.88	4.84

The *second* step involves associating different levels of shear strength improvement with the post-event traffic capacity of the bridges under study. We use different scenarios to describe the consequences of different post disasters and further assume that the shear response would be varied under these scenarios. We generated 12 random scenarios, each of which is 10% varied from the original nonlinear relationship curve in Figure 3.6.

Let $\Delta F_{nonlinear}$ be the shear strength improvement using results from lower level. The relationship is described as equation (3-10).

$$\Delta F_{nonlinear} = -0.0856w^2 + 2.8442w - 0.3227 \quad (3\text{-}10)$$

The next step involved connecting the shear strength improvement with the link traffic capacity. Denote θ as the relationships between shear strength improvement and steel thickness, which contains a set of traffic capacity ratios that can be obtained by dividing the link post-disruption capacity over its original capacity. We assume that the post-disruption traffic capacity has at least κ% of original capacity (e.g., $\kappa = 20$). Then, the parameter θ is a fractional value between κ% and 1, which can be obtained using shear strength improvement $\Delta F_{nonlinear}$ in equation (3-10). Let $\Delta \mathrm{F}_{max}$ be the maximum allowable shear strength improvement, beyond which the improved shear strength has no further impact on link traffic capacity. The shear strength improvement is then connected to traffic capacity via equation (3-11).

$$\theta_{nonlinear} = min(\frac{\Delta F_{nonlinear}}{\Delta \mathrm{F}_{max}} * 0.8 + 0.2, 1) \qquad (3\text{-}11)$$

A "lookup table" of showing the relationship between θ and retrofit strategies can be obtained. There are 12 lookup tables, each of which describes one of 12 scenarios.

Baseline results: The results of the baseline study, presented in Table 3.3, includes the costs, solution performance, and selected strategies (presented in rows) under different budget levels (i.e., \$30m, \$60m and \$90m presented in columns). The top section of the table reports various costs. In particular, the objective value is the summation of CVaR and the total expected cost, which is further decomposed to retrofit cost and expected travel cost. The solution performances of the GBD's solution time, optimality gap, and iterations are reported in the middle section of the table. We used a generalized Benders decomposition algorithm to solve the upper level problem as we described in section 3.3.

The optimality gap shows the convergence of the algorithm, which reflects the high quality solutions by the algorithm. The computing times and iterations indicate the efficiency of the algorithm. The bottom section explicitly details the optimal strategies applied to different bridges.

Table 3.3 Network level results by integrating both levels

	Budget Levels		
	\$30M	\$60M	\$90M
Obj. Value (10^6)	732.036	680.703	667.132
CVaR (10^6)	368.738	343.099	335.833
Total Exp. Cost (10^6)	363.298	337.604	331.299
Retrofit Cost (10^6)	29.360	50.560	83.840
Exp. travel cost (10^6)	333.938	287.044	247.459
CPU Time (mins)	9.25	37.22	55.57
Optimality Gap	0.50%	0.82%	0.57%
# of Iteration	13	45	74
Bridge A Strategy	h2	h4	h4
Bridge B Strategy	h1	h2	h2
Bridge C Strategy	h0	h0	h1
Bridge D Strategy	h0	h2	h3

We can see that as the increase of the total available budget, the expected travel cost, CVaR value and objective value decrease. This is because higher budget allows for the use of enhanced retrofit strategies, which are clearly indicated in Table 3.3. As a result,

the structural performance is enhanced in support of traffic throughput and the network becomes more resilient. The model gets more difficult to solve with the increase of budget levels, which requires more CPU times and number of iterations. This is because more feasible solutions become available for the first stage variables due to the raised budget.

Comparisons with other cost estimation methods: We compared the results of proposed bi-level model with linear cost estimation and engineering practice. Linear cost estimation is derived by substituting equation (3-10) into equation (3-11), then taking derivative of $\theta_{nonlinear}$ with respect to w. The slop of linear relationship uses the gradient of nonlinear curve at w=0. As link post-disruption traffic capacity cannot exceed the maximum traffic capacity, θ_{linear} is always less than or equal to 1. In addition, engineering practice, an index based method, prioritizes bridges according to the severity of expected damages of bridges, which is widely used in reality due to its easy implementation. Following different cost estimations, the θ values vary. For risk-averse decision makers, the bridge to receive retrofits is ranked according to the severity of damage and the one that is ranked highest may be retrofitted to its maximum possible performance within budget. The remaining budget if any will then be used to retrofit bridge ranked second highest. It continues until budget is depleted. In this subsection, we will explore the effects of cost estimations on the strategic solution and system performance.

The network-level results of engineering practice and solutions based on linear cost estimation are provided in Table 3.4, for comparison with the results of our nonlinear cost

estimation (copied from Table 3.3). The model will be run separately for both nonlinear and linear sets of θ. After obtaining retrofit decisions using linear set of θ, we evaluate system performance of the linear cost estimation decisions by re-running the model under nonlinear set of θ. For different cost estimations and engineering practice, we consider three different levels of budget level at \$30M, \$60M and \$90M. As similarly structured, Table 3.4 reports both costs and retrofit strategies. For linear cost estimation, we first run the model using θ_{linear} values to obtain retrofit decisions (strategies for all bridges), and then evaluate the performances of retrofit decisions under the nonlinear estimations. For engineering practice, we first rank bridges according to the severity of damages, which is in the order of bridges C, B, D, and A, and then determine the appropriate retrofit strategies for each bridge within budget. We then evaluate the solutions using the nonlinear cost estimations.

Table 3.4 Comparisons of proposed model with other methods

	Nonlinear			Linear			Engineering Practice		
Budget	$30M	$60M	$90M	$30M	$60M	$90M	$30M	$60M	$90M
Obj. Value (10^6)	732.036	680.703	667.132	732.036	680.703	667.705	846.350	979.068	1038.614
CVaR (10^6)	368.738	343.099	335.833	368.738	343.099	336.147	426.536	494.207	523.967
Total Exp. Cost (10^6)	363.298	337.604	331.299	363.298	337.604	331.558	419.814	484.861	514.647
Retrofit Cost (10^6)	29.360	50.560	83.840	29.360	50.560	80.000	29.360	56.400	87.120
Exp. travel cost (10^6)	333.938	287.044	247.459	333.938	287.044	251.558	390.454	428.461	427.527
Bridge A Strategy	h2	h4	h4	h2	h3	h3	h0	h0	h0
Bridge B Strategy	h1	h2	h2	h1	h2	h2	h1	h0	h0
Bridge C Strategy	h0	h0	h1	h0	h0	h1	h0	h2	h4
Bridge D Strategy	h0	h2	h3	h0	h2	h2	h2	h4	h4

From the results, the strategies under the budget levels of $30M and $60M are identical. However, the strategies for bridge A and bridge D changed under the budget level of $90M. As the linear cost estimation is more optimistic compared to the nonlinear counterpart, the retrofit cost under linear cost estimation ($80M) is slightly lower than the nonlinear cost estimation ($83.84M). However, the less retrofitted bridge network because of lower traffic capacity may cause higher travel cost, although the total cost (including retrofit, travel, and risk consequence) is almost identical. In general, there are trivial changes between the linear and nonlinear estimations under all budget levels. That is because the retrofit costs we use may lead to similar retrofit decisions at certain budget level for both estimations, and further result in similar network performance.

A comparison of the differences between linear and nonlinear cost estimations shows more substantial than the differences between engineering practice and nonlinear cost estimations. The network performance is worse even with a higher retrofit cost. The retrofit strategies for all bridges changed at all budget levels, because according to engineering practice, bridge C should be retrofitted first, which however, has the most expensive retrofit schemes based on Table 3.2. Furthermore, the network performance by engineering practice worsens with the increase of budget levels. This degradation in network performance is due to an increase in budgets, which will in turn incur the use of more expensive strategies on less important bridges and less expensive strategies on more important bridges. Therefore, more budgets do not guarantee less total costs in engineering practice. The results indicate that using the proposed model will outperform engineering practice when considering post-event traffic flow and network impact.

5. Conclusions

We developed a novel, infrastructure-retrofit decision program based on a bi-level optimization framework, which simultaneously takes the network effects and individual structural enhancement in a single framework. In particular, the upper-level problem was essentially a network design problem, which determines the best retrofit resource allocations among different at-risk structures and the lower-level problem aims to improve the bridge's traffic capacity under the budget. The resulting retrofit strategy and bridge's traffic capacity were returned to the upper-level problem for determining the network performance.

At the lower level framework, we use different dimension of steel jacketing applied on the bridge pier to reflect different retrofit levels. Using bridge pier retrofit as example, we established a nonlinear relationship between structural performances and retrofit levels for bridge retrofit designs with the help of FE models. This relationship was then converted into a traffic capacity-cost relationship and used as a design guide for selecting optimal highway bridge retrofit alternatives at upper level framework. The two levels of the modeling framework were combined, which in turn yielded different resource allocation strategies at the upper level with the different assumptions of bridge traffic capacity-cost relationships (e.g. the acquisition of a simple linear relationship and the nonlinear relationship from lower level framework). The proposed model was found to outperform engineering practice in terms of system costs when considering the overall effect of the transportation network. The differences between the engineering practice

and nonlinear cost estimations were more substantial compared to the differences between linear and nonlinear cost estimations. Also, increasing budgets does not lead to less total costs in engineering practice.

Consequently, additional research is needed to specify and enhance the realism of the lower level structural modeling assumptions. First, our model should be combined with a hazard generating component that uses more realistic disaster loading and model the rebar elements separately. Next, research should be undertaken to consider the robustness, which is a measure of retrofit design parameters uncertainty, to enhance the robust nature of the problem. Naturally, our network level modeling established must be combined with the new lower level models to achieve that enhanced criteria.

Chapter 4 Two-Stage Minimax Regret Robustness of Bridge Network Protection Integrating Earthquake Simulations

1 Introduction

Bridge failures due to disasters such as earthquakes, will affect traffic conditions and change traffic patterns dramatically as in the collapse of I-35W Mississippi River Bridge and San Francisco-Oakland Bay Bridge. The traffic served by the bridges was diverted to alternative routes, causing considerate amount of congestions in nearby areas. The drivers had to take routes with longer driving distance and travel time in order to avoid heavy traffic congestions.

Although transportation network protection against uncertain future disasters has been a subject of long-lasting interest for researchers and practitioners, the literature has its limitation. In the perspective of transportation planners and engineers, traffic user behaviors and traffic disruptions due to earthquake are normally considered, but simple assumptions are usually made on the bridge retrofit cost and corresponding post-earthquake structural conditions. On the other hand, in the perspective of structure engineers, they consider individual infrastructure retrofit design and rank the priority of retrofit decisions by bridge damage conditions, or they only consider retrofit designs for simple network configuration without traffic disruptions. Decisions made at network level determine a retrofit strategy for each bridge, i.e., determine the amount of resource

allocated to each bridge; decisions made at infrastructure level determine how to use the resource allocated to a given bridge, i.e., choose a specific retrofit design, which affects bridge post-earthquake conditions, thus further affects traffic at network level. Both levels decisions should be considered jointly because the two systems interact with each other.

Handling uncertainty is a modeling challenge to the proposed modeling framework. A discrete set of scenarios are used to approximate the earthquake events. An engineering practice is to examine all possible scenarios and forms a set of scenario-specific solutions or policies. Since future events are unknown at the time of making decisions, it would be impossible for us to determine which policy to implement. Even if a representative scenario could be identified, the best policy for this representative scenario may not perform well or even be feasible for other scenarios. Normally, stochastic programming and robust optimization methods are applied to generate decisions considering all scenarios. Stochastic programming method overlooks extremely low probability scenarios, which may have devastating results in disaster management. Robust optimization, on the other hand, aims to optimize problem with worst-case scenarios but provides solutions that are often considered conservative. In this study, I use a minimax regret criterion, an alternate way of making decisions in decision theory that provides less conservative solutions compared to robust optimization (Inuiguchi & Sakawa, 1995). Regret is measured by total cost deviation between current solution without future information and perfect-information solution (we know which scenario will occur in future). Minimax regret approach has been applied to a number of engineering fields,

including transmission expansion planning (Chen, et al., 2014), wind power unit commitment (Ruiwei, et al., 2013), and uncapacitated lot-sizing (M. Zhang, 2011). By applying the minimax regret criterion, the solution that maximizes the worst-case regret over all possible scenarios can be obtained.

The contributions for this study are bi-fold. The first contribution is the integration of seismic analysis into decision making process. Previously, earthquake scenarios are generated using assumed post-earthquake bridge damage conditions (Fan, et al., 2010). However, since structures have complex behavior when subject to earthquake excitation, it is more realistic to evaluate the bridge damage by considering dynamic response and seismic performance. By developing a Pareto front of cost-safety-robustness, one can identify a small number of preferred retrofit designs and construct a set of retrofit strategies to be used in the network level mode. Another contribution is the development of a new formulation using minimax regret criterion, which provides solutions with certain level of robustness but less conservative compared to robust optimization method.

The research efforts lie in the integration of the earthquake simulations for bridge seismic response and network resource allocation model, which is essential to make realistic and efficient retrofit decisions on both network level and structure level. For the earthquake simulations, multiple earthquake ground motions have been used as seismic loads to simulate bridge damages due to earthquakes. Finite element analysis at infrastructure level will then apply the seismic loads to bridge columns to assess bridge damages and provide information on the relationship of bridge damages and retrofit cost.

The cost-damage relationship will then be used in network level transportation models to reflect the disturbance of earthquakes on traffic. At network level, I developed a two-stage minimax regret model for transportation network resource allocation problem. Multiple retrofit alternatives and multiple bridge damage states are integrated into the network level model that would make the decision making process more flexible and realistic.

2. Literature review

Previous research efforts on bridge retrofit studies, based on their goals, can be categorized by maximizing network post-disaster capacity, maximizing the reliability of the transportation network and minimizing post-earthquake system travel delays.

Studies that aim to maximize network capacity normally focus on short term economic effects for post-disaster evacuations. Lee, et al. (2011) used a non-sampling method to estimate post-earthquake network capacity considering bridge deteriorating process. The network capacity, indicated by the maximal flow from downtown areas to evacuation areas, is estimated using maximal flow analysis. The fragility or the likelihood of damage of the bridges was estimated through simulation or bridge columns subject to local pseudo-spectral acceleration at bridge locations. Liang Chang, et al. (2012) presented an OD-independent method to calculate post-earthquake transportation network evacuation capacity. They solve a maximum flow network design problem for each earthquake

scenario and aggregate the results to provide a retrofit program by cost effectiveness analysis.

Network reliability is defined as the probability that the network remains its connectivity and functionality over a given period of time. Connectivity depends on the post-earthquake network completeness, thus is a suitable goal for short term emergency response and providing humanitarian aid. A pioneer study, presented by Augusti, et al. (1998), provided a reliability based method to prioritize the maintenance strategies for deteriorating bridges in a simple series-parallel system. M. Liu and Frangopol (2006) provided a bridge network maintenance method that considered time-dependent structural reliability prediction, highway user cost and bridge life cycle cost. However, they assumed that there is no correlation among bridge failures, and used unrealistic same traffic pattern for all scenarios. Bocchini and Frangopol (2011) assessed network life-cycle performance and used a time variant reliability model for individual bridge. They performed transportation network analysis for every combination of bridge service states in a small six-node network. System travel delay is one of the most commonly used system performance metrics for transportation networks. It provides information on highway user costs and is suitable for evaluating long term economic effects. This metric has been widely used to assess seismic impacts on transportation networks.

Many studies fall into the third category more focus on structural engineering perspective. They have detailed disaster modeling component but simplified transportation network. Shinozuka, et al. (2003) estimated the effects of pre-earthquake

retrofit and post-earthquake repair on driver delays. They used probability based fragility curves to generate initial damage states of bridges and used hypothetical probability curve for repair completion time. The effectiveness of retrofit is reflected by enhanced fragility curves with less physical damages. Zhou, et al. (2004) also used bridge fragility curves and extended their work through cost-benefit analysis of retrofit different cases. Five retrofit cases were presented, each with different percentages of bridges being retrofitted. The decision was to select one retrofit case with certain percentage of bridge being retrofitted without identifying which bridges receive retrofit. That is because the retrofitted bridges were randomly selected by simulation. Sohn, et al. (2003) analyzed the economic impact of earthquakes on transportation networks for a single earthquake scenario. They used fragility curves to generate bridge damage states and integrated a traffic demand loss function. Retrofit priority for links in transportation network was established by using benefit-cost analysis. Zhou, et al. (2010) conducted a simulation based study to assess social economic effect of seismic retrofit of bridges. They generated a set of earthquake scenarios and simulated the damages with and without retrofit. Retrofit decision can be made for either retrofit all bridges or not by conducting cost-effectiveness analysis.

Determining optimal retrofit decisions needs many assessments of network level performance and it would be impossible to find optimal retrofit decisions without efficient computational algorithm. Some studies focus more on finding efficient algorithms to optimize retrofit decisions with assumed bridge damage conditions after earthquake. C. Liu, et al. (2009) developed a generalized Benders decomposition solution

method to determine bridge retrofit program with binary retrofit decisions and binary damage states for each bridge. Furuta, et al. (2011) used genetic algorithm to optimize inspection and repair plan for bridges under seismic risk in a network with multiple conflicting objectives. A recent study by Brown, et al. (2013) used dynamic traffic assignment algorithm to assess post-earthquake network performance and integrated an infrastructure model to evaluate post-event infrastructure condition. More focused on short time post-event evaluation, they considered multiple objectives, including total peak period travel time, travel time to hospital and retrofit cost, to select optimal retrofit strategy.

3. Methodologies

The objective of this proposed study is to develop a robust modeling framework and solution method to improve resilience and sustainability of transportation infrastructure system under earthquake uncertainty. First, I will present the methodology framework for the whole study in section 3.1. Formulations for network level model will be discussed in section 3.2. In sections 3.3, earthquake simulation method will be discussed.

3.1 Methodology framework

The methodology framework is shown in Figure 4.1. First, a set of earthquake scenarios, which are represented by different ground motions, are chosen as inputs for

seismic analysis. Then, an infrastructure assessment component is developed using finite element models with different retrofit designs. The results of seismic response will be aggregated by retrofit designs across different earthquakes to generate a cost-safety-robustness Pareto front to select a set of preferred strategies for network level model. The next step is to generate bridge damage scenarios. Using the preferred strategies, we connect the structural system performance to traffic capacity and generate bridge damage scenarios which are represented by a parameter called the ratio of post-earthquake link capacity $\theta_a^{h,k}$. A mean-risk network design model using minimax regret criterion will aggregate all bridge damage scenarios and provide a retrofit strategy for each bridge in the transportation network. If the strategy combinations results in system optimal at network level, one can claim that the best retrofit strategies are found, otherwise the network model will select another strategy for bridges.

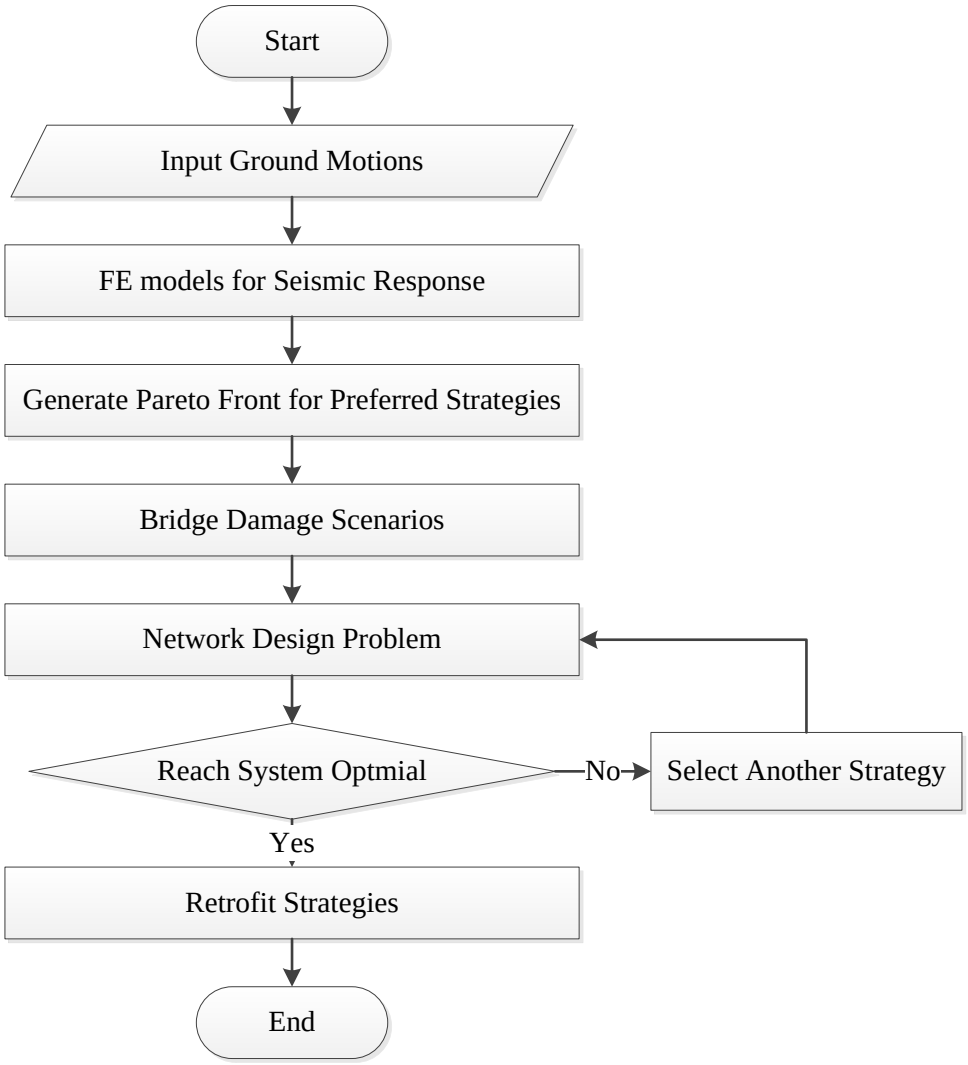

Figure 4.1 Methodology framework

3.2 Upper level subproblem: resource allocation problem over network

A spatially distributed transportation network can be represented by a network consists of a set of nodes and connecting links. Denote the transportation system by a directed network flow graph $G(N, A)$. The links in this study are classified as road links and bridge links. Bridge links, denoted by $\overline{A}$ ($\overline{A} \subset A$), $\left|\overline{A}\right| = \overline{m}$, are the set of links subjecting to seismic hazards, where the link capacities may be reduced after earthquake. Road links, denoted by $A \backslash \overline{A}$, are the links assumed to be intact with post-earthquake capacities unchanged. Retrofit decisions are made before uncertainty is revealed. Once the decisions are made, they cannot be changed because retrofit decisions are capital intense. The retrofit decisions are bi-fold, consisting of the amount of resources to be allocated to each bridge and optimal retrofit schemes applied to individual bridge using the allocated resource.

In this study, scenarios are defined as combinations of different bridges damage conditions in the network. Each scenario is associated with an occurrence probability. Let k describe a scenario with corresponding probability p^k. Let K denote a set of earthquake events, $k \in K$. We assume that the selected retrofit decision variable ($u_a^h = 1$) will affect the post-earthquake bridge capacity $\hat{c}_a^k$, that is $\hat{c}_a = c_a \sum_{h \in H} u_a^h \theta_a^{h,k}$, where c_a is the bridge traffic capacity before earthquake, and $\theta_a^{h,k}$is a parameter describing the post-earthquake link capacity ratio which is estimated by the maximum lateral displacement of a reinforced concrete (RC) bridge pier at center of inertia for a given earthquake ground motion k.

In the field of transportation system analysis, traffic networks are assumed to follow two typical conditions, user-equilibrium (UE) and system-optimization (SO) (Yang & H. Bell, 1998). Since the focus of this study is on the long term economic effect of retrofit decisions, it is assumed that traffic flow is controlled by a central planner to achieve SO condition.

The network level model is a network design problem that aims to minimize retrofit cost and second stage costs. The retrofit cost, which is the first stage cost, is incurred at the design of infrastructure rehabilitation schemes. We assume that more robust designs are more costly. The retrofit cost determines the money can be spent in retrofit design of infrastructure at lower level framework. The second stage cost consist of costs associated with system travel delays due to congestion and unmet travel demand cost. The system travel time can be estimated by modeling traffic flow distribution and travel time over highway networks through the traffic assignment step of four-step transportation forecasting process (McNally, 2008). The system travel time can be expressed as $\sum_{a\in A} v_a^k t(v_a^k)$, where v_a and $t(v_a^k)$ represent post-earthquake travel flow on link a and travel time on link a for scenario k, respectively. The flow v_a^k is expressed in passenger car unit for daily peak hour. The link travel time $t(v_a^k)$ is expressed in hours. The system travel time is estimated in hours for daily peak hour and is converted to money value using conversion parameter $\beta = VOT \times p$, where VOT is the value-of-time and p is the number that convert peak hour flow to average daily traffic.

In the network level model, post-earthquake travel demand is allowed to be unsatisfied due to high travel cost. There are various reasons for high travel cost, such as totally or partially shutdown of certain roadways, and drastic increase of traffic congestion in the network. The unsatisfied demand d will be penalized by a big M factor, thus the cost associated with unsatisfied demand can be expressed as Md^k.

For fixed earthquake scenario k, the network design problem (NDP) can be expressed as:

$$\text{(NDP)} \quad min_{u,v,x,d} \sum_{a\in A}\sum_{h\in H} c_a^h u_a^h + \gamma \sum_{a\in A} v_a^k t(v_a^k) + M \sum_{r\in R, s\in S} d^{rs,k} \tag{4-1}$$

$$s.t. \quad c^T u \le B \tag{4-2}$$

$$\sum_{h\in H} u_a^h = 1, \ \ \forall a \in \bar{A}, \tag{4-3}$$

$$W x^{rs,k} = q^{rs} - d^{rs,k}, \ \ \forall r \in R, s \in S, \tag{4-4}$$

$$v_a^k = \sum_{r\in R}\sum_{s\in S} x_a^{rs,k}, \ \ \forall a \in A, \tag{4-5}$$

$$t(u,v,k) = t_0[1 + \beta(\frac{v_a^k}{\hat{c}_a^k})^4], \forall a \in A, \tag{4-6}$$

$$with \quad \hat{c}_a^k = \begin{cases} \sum_{h\in H} u_a^h \theta_a^{h,k} c_a, \forall a \in \bar{A} \\ c_a, \forall a \in A \backslash \bar{A} \end{cases}, \tag{4-7}$$

$u \in \{0,1\}^{|A|\times|H|}$, $x \in \mathbb{R}_+^{|A|\times|R|\times|S|\times|K|}$, $v \in \mathbb{R}_+^{|A|\times|K|}$, $d \in \mathbb{R}_+^{|R|\times|S|\times|K|}$.

The objective (4-1) aims to minimize the retrofit cost, travel delays, unsatisfied demand penalty and repair cost. Adding unsatisfied term ensures there is no feasibility

issues for any first-stage decision u. Constraint (4-2) ensures that the retrofit cost does not exceed available budget. Constraints (4-3) and $u \in \{0,1\}^{|\bar{A}|\times|H|}$ ensure only one strategy can be selected for each bridge. Constraints (4-4) ensure flow balance for all nodes in the network. Constraints (4-5) aggregate link flow for each origin-destination (OD) pair to actual link flow. Constraints (4-6) are the Bureau of Public Roads (BPR) functions(Bureau of Public Roads, 1964) which are conventional functions used in transportation engineering that describe link flow and link travel time relationship. Constraints (4-7) describe post-earthquake capacity for bridge links and road links, where I assume that the roads are intact after earthquake. NDP is mixed integer nonlinear program where the nonlinearity comes from the BPR function. Let $\mathcal{Q}(k)$ be the optimal objective value for NDP. Since the first stage decision u is made under a specific scenario k, $\mathcal{Q}(k)$ represents perfect-information total cost.

For brevity, let u denote first-stage binary variables, $u \in \{0,1\}^{|\bar{A}|\times|H|}$, I group all second-stage continuous variables to be x with dimension n, $x \in \mathbb{R}_+^n$. Let $c(u)$ be the retrofit cost in (4-1). Let $f(u,x)$ denotes all other costs in the objective (4-1) except retrofit cost. Then, an abstract transportation network protection model for fixed future scenario k can be expressed as:

$$\mathcal{Q}(k) = \min_{(u,x)\in\mathcal{M}(k)} c(u) + f(u,x), \tag{4-8}$$

where $\mathcal{M}(k) \coloneqq \{(u,x) \in \{0,1\}^{|\bar{A}|\times|H|} \times \mathbb{R}_+^{|R|\times|S|\times|K|}$:

$$g^k(u,x) \leq 0, \tag{4-9}$$

$$h^k(u,x) = 0, \tag{4-10}$$

$$\sum_{h\in H} u_a^h = 1, \forall a \in \bar{A}.\}$$

Constraint set (4-9) represents all inequality constraints; Constraint set (4-10) represents all equality constraints; $\mathcal{M}(k)$ is the feasible region of u and x fixing scenario k.

For fixed first-stage decision variable u, the maximum regret is defined as:

$$Reg(u) \coloneqq \max_{k\in K}\{\min_{(u,x)\in\mathcal{M}(u,k)}\{c(u) + f(u,x)\} - \mathcal{Q}(k)\} \tag{4-11}$$

where $\mathcal{M}(u,k)$ is the feasible region of second-stage variables x given fixed earthquake scenario k and retrofit decision u.

By definition, $\min_{x\in\mathcal{M}(u,k)}\{c(u) + f(x)\}$ provides total cost by adjusting second-stage variables for fixed retrofit decision u and realized earthquake scenario k. $\mathcal{Q}(k)$ is the total cost of perfect-information solution for scenario k. In this study, the maximum regret $Reg(u)$ is minimized by selecting the best first stage retrofit decision u across all scenarios.

$$\text{(MRP)} \quad \min_u Reg(u) \tag{4-12}$$

$$\text{s.t.} \quad \text{(4-9), (4-10) and } u \in \{0,1\}^{|\bar{A}|\times|H|}.$$

The above formulation is called Minimax Regret Problem (MRP).

3.3 Lower level subproblem: develop a Pareto front for cost-safety-robustness relationship and generate bridge damage scenarios

The lower-level problem is to derive a Pareto front for cost-safety-robustness relationship of retrofit strategies using seismic response results. Then we identify a set of preferred strategies from the Pareto front to be used in network level model. The relationship between retrofit cost and bridge's traffic capacity is then identified to generate bridge damage scenarios.

There are several steps to derive the Pareto front for cost-safety-robustness relationship which is illustrated with a flowchart shown in Figure 4.2. First, we define the seismic retrofit problem and classified the design parameters. We specify the design domain and choose a set of earthquake scenarios, represented by different ground motions, as inputs for seismic analysis. The design domain is specified in discrete number for the consideration of construction which consists of a set of M designs. Then, for each design, a nonlinear finite element model is developed with a specific combination of design parameter values. Each model is then tested with a set of N ground motion records in the inner loop to obtain seismic response. The next step represented by the outer loop is to repeat the analysis for each of M designs in the design space. In the following step, the problem can be seen as a multi-objective optimization considering multiple design criteria. There are two different measures, the safety and robustness measures, can be generated from seismic response. As each retrofit design is associated with a cost, once we obtain the measures, a three dimensional Pareto front for cost-safety-robustness relationship can be derived. A set of non-dominated solutions may be obtained

which means there may be tens of even hundreds of plausible designs. We then use a new measure to identify several preferred strategies from the whole design space in order to be used by the network level model.

Note that computationally evaluating structural seismic performance given retrofit design is a generic process. It can be applied to any bridge types or bridge component. One important aspect that needs attention is the indicator of safety and robustness. In our case study, we use max lateral displacement for safety measure and use the standard deviation of the max lateral displacement across different earthquake scenarios for robustness measure. However, one can always use many other aspects of the bridges and choose other indicators for the above measures.

The next step is to generate bridge damage scenarios. Bridge damage scenarios are represented by a ratio of post-earthquake link capacity $\theta_a^{h,k}$. The generating process requires the connection between structural performance and traffic capacity as well as the cost structural performance relationship. For the set of preferred strategies, we select safety measure to be structural performance. Using the same technique describe in chapter 3, we connect structural performance to traffic capacity by associating the structural performance to traffic capacity proportionally. We set a minimum traffic capacity for the bridge link and a maximum traffic capacity after earthquake which is the original traffic capacity of the bridge link. Finally, we can evaluate relationship between the traffic capacity and retrofit cost for each earthquake and obtain the ratio of post-earthquake link capacity which will be used as an input for upper level model.

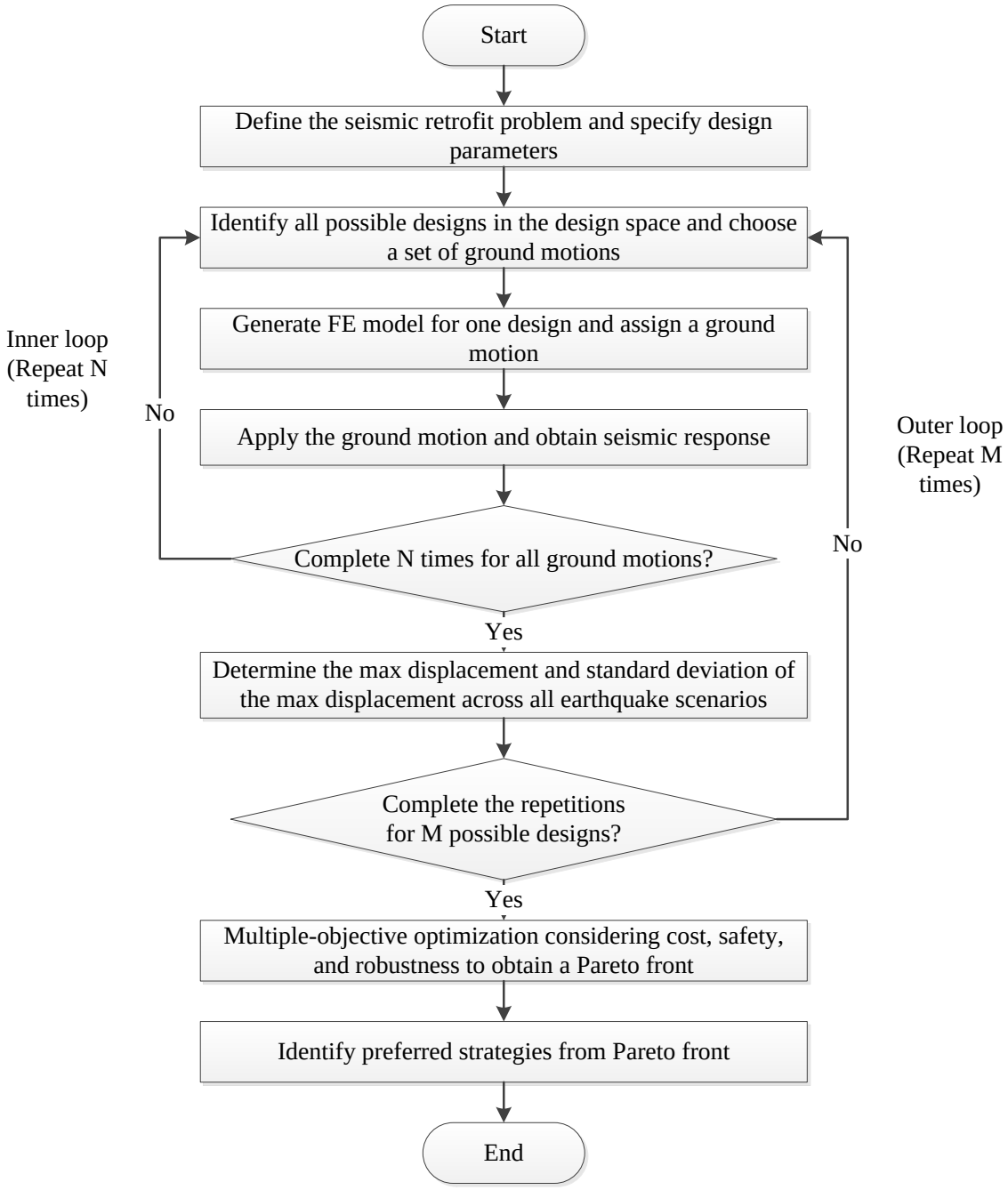

Figure 4.2 Flowchart on the robust design of bridge seismic retrofit problems

4. Solution methodology

In this section, a cutting plane based decomposition method is developed to solve the network level problem MRP. First, by using the strong duality theory, one can reformulate the maximum regret $Reg(u)$ in the objective function on which to apply cutting plane method.

Let μ^k and ν^k represent the Lagrangian duals associated with (4-9) and (4-10) respectively.

$$Reg(u)$$

$$= c(u) + \max_{k\in K}\{\min_{x\in\mathcal{M}(u,k)}\{f(u,x)\} - Q(k)\} \tag{4-13}$$

$$= c(u) + \max_{k\in K}\left\{\max_{(\mu^k,\nu^k)\in\mathcal{D}(u,k)}\{f(u,x) + (\mu^k)^T g^k(u,x) + \nu^k h^k(u,x)\} - Q(k)\right\} \tag{4-14}$$

where (4-13) takes retrofit cost $c(u)$ out of inner problem, (4-14) takes strong duality, $\mathcal{D}(u,k)$ is the dual feasible region.

By introducing a scalar ϕ, problem MRP can be written as

$$\min_u \quad \phi$$

$$\text{s.t.} \quad \phi \geq c(u) + T^k, \forall k \in K$$

$u \in \{0,1\}^{|\bar{A}|\times|H|}$.

where $T^k = \max_{(\mu^k,\nu^k)\in\mathcal{D}(u,k)}\{f(u,x) + (\mu^k)^T g^k(u,x) + \nu^k h^k(u,x)\} - \mathcal{Q}(k)$

s.t. (4-9) and (4-10)

Let $U \coloneqq \{u|u \in \{0,1\}^{|\bar{A}|\times|H|}, c^T u \le B, \sum_{h\in H} u_a^h = 1, \ \forall a \in \bar{A}\}$. The regret master problem can be written as:

Regret Master problem (Regret MP)

$\min_u \phi$

s.t. $u \in U$

Optimality cut $\phi \ge c(u) + Q^k(u) - \mathcal{Q}(k), \ \forall k \in K, l \in L$.

The corresponding regret sub problem for scenario k can be written as:

Regret Sub problem Q^k (Regret SP-k)

$min_{v,x,d} Q^k(\bar{u}) = min_{v,x,d}\gamma[v^T t] + M\sum_{r\in R,s\in S} d^{rs,k}$

s.t. $Wx^{rs,k} = q^{rs} - d^{rs,k}, \ \forall r \in R, s \in S,$

$v_a^k = \sum_{r\in R}\sum_{s\in S} x_a^{rs,k}, \ \forall a \in A,$

$$t(u,v,k) = t_0[1+\beta(\frac{v_a^k}{\hat{c}_a^k})^4]\,, \forall a \in A,$$

$$\textit{With} \quad \hat{c}_a^k = \begin{cases} \sum_{h\in H} u_a^h \theta_a^{h,k} c_a\,, \forall a \in \bar{A} \\ c_a, \forall a \in A\backslash\bar{A} \end{cases},$$

$$u \in \{0,1\}^{|A|\times|H|},\ x \in \mathbb{R}_+^{|A|\times|R|\times|S|\times|K|},\ v \in \mathbb{R}_+^{|A|\times|K|}, d \in \mathbb{R}_+^{|R|\times|S|\times|K|}.$$

The Regret SP-k is a nonconvex nonlinear problem with given first stage variable $\bar{u}$. By using reformulation technique described in (Lu, et al., 2015), we can get a convex formulation of Regret SP-k:

Convex Regret SP-k

$$\min_{v,x,d} Q^k(\bar{u}) = \min_{v,x,d} \gamma \left[\sum_{a\in\bar{A}} t_{0a}(v_a^k + \beta y_a^k) + \sum_{a\in A\backslash\bar{A}} t_{0a}(1+\beta(\frac{v_a^k}{c_a})^4) \right] + M \sum_{r\in R, s\in S} d^{rs,k}$$

s.t. (4-4) - (4-5)

$$(v_a^k)^5 \le \sum_h z_a^{h,k} \left(\theta_a^{h,k}\right)^4 c_a^4, \forall a \in \bar{A}, k \in K \tag{4-15}$$

$$z_a^{h,k} \le \bar{y} u_a^h, \forall a \in \bar{A}, h \in H, k \in K \tag{4-16}$$

$$y_a^k = \sum_{h\in H} z_a^{h,k}\,, \forall a \in \bar{A}, k \in K. \tag{4-17}$$

where $\bar{y} = \frac{(\bar{v}_a)^5}{\left(\theta_a^{h,k}\right)^4 c_a^4}$ and $\bar{v}_a = \varsigma c_a$ is the upper-bound traffic volume of link a, and ς is a sufficiently large number.

Let $\bar{u}^l$ be the optimum solution of the master problem at l^{th} iteration. Then the optimality cut for the l^{th} iteration is:

$$\phi \geq \sum_{a\in\bar{A}} \sum_{h\in H} c_a^h u_a^h + \sum_k Q^k(\bar{u}^l) - \mu^{kl}\bar{y}(u - \bar{u}^l) - Q(k) \qquad (4\text{-}18)$$

where μ^{kl} is the dual variable vector associated with (4-16).

The regret problem decomposition algorithm procedure:

1. Initialization $l = 0$, obtain perfect information solution $(\bar{u}_k, \bar{x}_k)$ for each scenario k.

   Calculate perfect-information total cost $Q(k)$ using $(\bar{u}_k, \bar{x}_k)$.

2. Solve the **Regret MP**.

   Let $(\overline{u}, \bar{\phi})$ be optimal solution.

3. Solve the **Convex Regret SP-k** for all scenarios. Set $l = l + 1$:

   Calculate $\phi^* = c(\overline{u}) + max_k(Q^k(\overline{u}) - Q(k))$.

4. The procedure terminates if the optimality gap $|1 - \frac{\overline{\phi}}{\phi^*}| \leq \varepsilon$ (ε is a predefined small value) is met. Optimal solution is found. Otherwise, add optimality cut to the regret master problem, and go back to step 2.

5. Numerical examples

Numerical examples are then used to demonstrate the minimax regret problem by integrating earthquake simulations. The structural assessment at the lower level is discussed and illustrated by a bridge pier example using a set of ground motion records for seismic response. The Pareto front is generated to illustrate the relationship between cost, safety and robustness. Preferred strategies are then selected based on the Pareto front. The bridge damage scenarios are then generated using the preferred strategies and are used as an input for the network level mode.

5.1 Pier structural assessment for seismic response

In the case study, we consider the dynamic response characteristics of the reinforced concrete (RC) bridge pier subject to bilateral seismic excitation. In particular, we use the time history analysis and apply bilateral ground motions from different earthquakes at the bridge piers to simulate the shear failure mode. A typical bridge pier has fixed support at the bottom and consists of a base, a column, and an auxiliary mass at the top. We assume that all bridges in the network are RC bridges that consist of two spans and a single middle pier. The pier, therefore, can be seen as the critical part of the bridge that should retain a certain level of lateral displacement during earthquake to avoid brittle shear failure mode. Steel jacketing is selected as retrofit alternative for the bridge piers where the thickness of steel jacket and elasticity modulus for steel material varies across different retrofit strategies. Bridge pier with a specific retrofit design is subject to

different earthquakes results in multiple time history analysis. This process is repeated for all retrofit strategies are tested. We choose the maximum lateral displacement of bridge pier as the safety measure and choose the standard deviation of the maximum lateral displacement across all scenarios as the robustness measure. Once we obtained the seismic response of piers with different strategies, a Pareto front for cost-safety-robustness relationship can be derived. Then we select a set of preferred strategies from the Pareto front to be used in network level model. By associating each retrofit design with a specific cost, the relationship between retrofit cost and bridge's traffic capacity can be identified to generate bridge damage scenarios.

Specimen geometry

We developed a scaled version of a typical RC bridge pier using the ANSYS FE analysis software (ANSYS) where the geometry of the RC bridge pier is adopted from the work of Nishida and Unjoh (2004). A typical pier consists of a base, a column and a steel weight at the top of pier. The column has a square cross-sectional geometry with dimension of $600\ mm \times 600\ mm$, and a height of $2000\ mm$. The base has a rectangular cross-section with dimension of $1500\ mm \times 2300\ m$, and a height of $700\ mm$. The longitudinal reinforcement ratio for the pier is 0.95%. Steel weight is set up at the top of RC column as auxiliary mass such that the axial compressive stress at the bottom of the column is $1.0\ \mathrm{N/mm^2}$. The height from the bottom of column to the center of inertia is $3040\ mm$. The material properties for concrete and steel jacket are shown in Table 4.1.

Table 4.1 Material Properties

Material	Material properties	Value
Concrete	Elasticity Modulus	32.7 GPa
	Poisson's Ratio	0.2
	Density	2500 kg/m3
	Compressive Strength	27 MPa
Steel Jacket	Elasticity Modulus	180 GPa - 220 GPa
	Poisson's Ratio	0.3
	Density	7850 kg/m3
	Yield Strength	295 Mpa

Finite element model development

The three-dimensional element of SOLID45 is selected for the FE model. There are several assumptions associated with the model. The base of the pier is fixed to model a rigid foundation for a bridge pier, that is, all base nodes are restrained in three directions. The damping constant is assumed as 2% for all elements. Rayleigh damping is assumed for overall damping matrix. We calculate alpha damping and beta damping using the modal analysis results from (Nishida & Unjoh, 2004). The values for alpha damping and beta damping constants are 0.377171486 and 0.000619, respectively. The geometry of the bridge pier is shown in Figure 4.3. We use a hexahedral meshing for the RC bridge column with side length of $200\ mm$ for column and $400\ mm$ for base and steel mass.

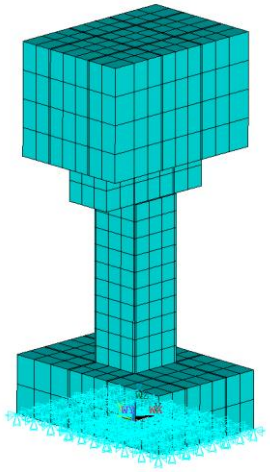

Figure 4.3 Bridge pier model

The steel jackets are used as strengthening material where steel plates are used to cover all four faces of the column. Different thickness of steel jacket and elasticity modulus are used to reflect different strategies. For convenience of construction, the design domain is specified in discrete number. The steel jackets have five different thickness values and five different values for elasticity modulus. We assume that the steel jacket is glued to the column specimen.

Ground motions

In our example, a set of 20 ground motions are selected for bridge pier seismic analysis. The ground motion set includes 10 records from historic earthquakes and 10 records from artificially-generated time history data (NISEE). Table 4.2 displays the ground motion records considered in this study.

Table 4.2 Ground motion considered

Ground Motion #	Earthquake	Earthquake Magnitude	Distance (km)
1	Tabas, 1978	7.4	1.2
2	Loma Prieta, 1989, Los Gatos	7	3.5
3	Loma Prieta, 1989, Lex. Dam	7	6.3
4	C. Mendocino, 1992, Petrolia	7.1	8.5
5	Erzincan, 1992	6.7	2
6	Landers, 1992	7.3	1.1
7	Nothridge, 1994, Rinaldi	6.7	7.5
8	Nothridge, 1994, Olive View	6.7	6.4
9	Kobe, 1995	6.9	3.4
10	Kobe, 1995, Takatori	6.9	4.3
11	Elysian Park 1	7.1	17.5
12	Elysian Park 2	7.1	10.7
13	Elysian Park 3	7.1	11.2
14	Elysian Park 4	7.1	13.2
15	Elysian Park 5	7.1	13.7
16	Palos Verdes 1	7.1	1.5
17	Palos Verdes 2	7.1	1.5
18	Palos Verdes 3	7.1	1.5
19	Palos Verdes 4	7.1	1.5
20	Palos Verdes 5	7.1	1.5

Pareto front for cost-safety-robustness relationship

The next step is to develop the Pareto front for cost-safety-robustness relationship. We first identify the design space where feasible design parameter values are determined. Different retrofit designs are associated with different retrofit costs. Then, time histories of response relative displacement are obtained for models with different retrofit designs and using different ground motion records. The safety and robustness measures can be generated from the time histories results considering across all ground motions. Thus, a Pareto front can be derived for cost-safety-robustness relationship.

We tested models with different thickness and different elasticity modulus values of steel jackets. We assume that the thickness of steel jacket w has five discrete design values, ranges from $25\ mm$ to $125\ mm$ and the elasticity modulus of steel jacket E_s also has five design values, ranges from $180\ GPa$ to $220\ GPa$. Each retrofit design consists of a combination of a steel jacket thickness value and an elasticity modulus values, i.e. there is 25 retrofit designs in total. Each design is associated with a specific cost. We assume that the retrofit cost c_r for a bridge with size $s_a = 1$ depends on the thickness and elasticity modulus values for steel jacket and the relationship is described in equation (4-13):

$$c_r = 80w(0.005E_s + 0.1) + c_l \tag{4-13}$$

where c_l is the labor cost and is set to be \$2M.

For each design and each ground motion, we record the time histories of response relative displacement of the two horizontal components at the center of inertia. For each response results, we choose the maximum of horizontal displacement at the center of inertia for both horizontal directions as the safety measure, i.e., higher maximum displacement value means less safety for a structure during earthquakes. The robustness measure, accounts for the effect of uncertainties from different earthquakes on the maximum displacement values, is defined as the standard deviation of maximum displacement for one design across different earthquakes. A smaller standard deviation stands for a greater robustness. By taking the maximum of the safety measure across all earthquakes, we can obtain the Pareto front for cost-safety-robustness relationship which is shown in Figure 4.4. When focusing on two dimensions, Pareto front for cost and max displacement relationship is shown in Figure 4.5, Pareto front for cost and standard deviation of max displacement relationship is shown in Figure 4.6.

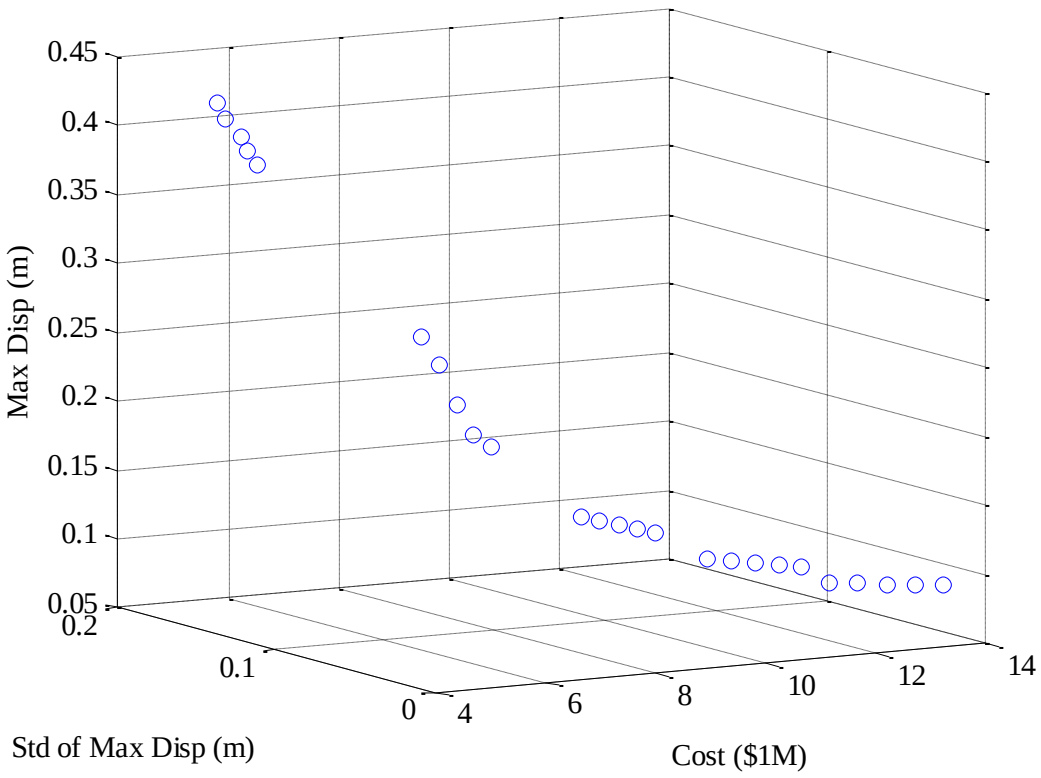

Figure 4.4 Pareto front for cost, max displacement and standard deviation of max displacement relationship

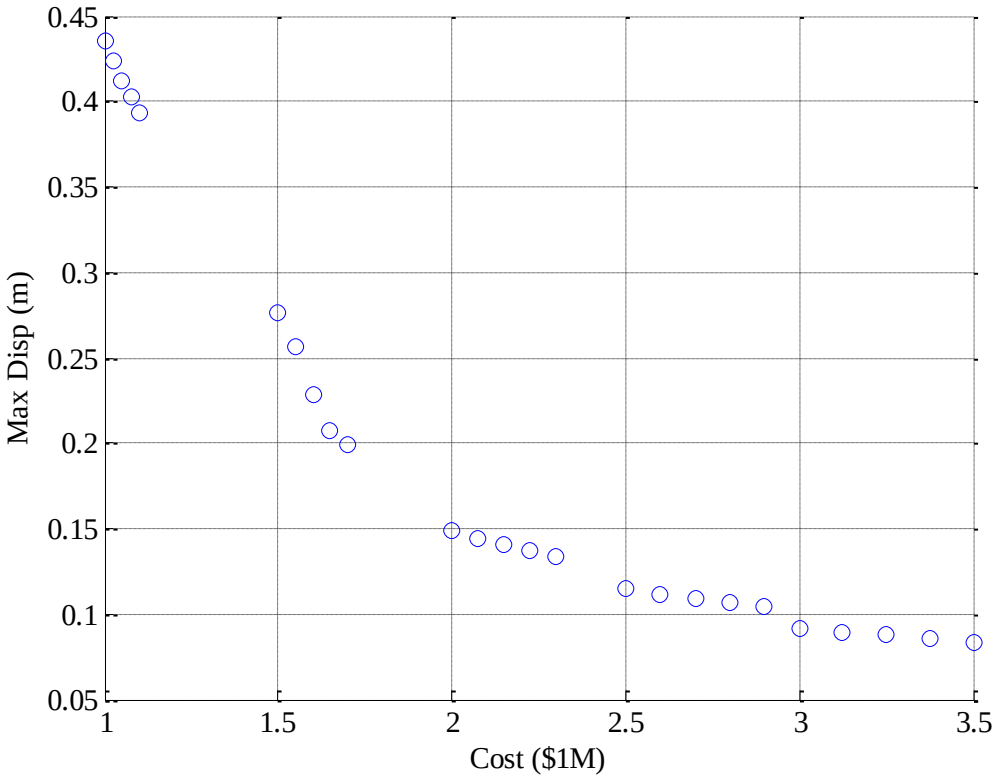

Figure 4.5 Pareto front for cost and max displacement relationship

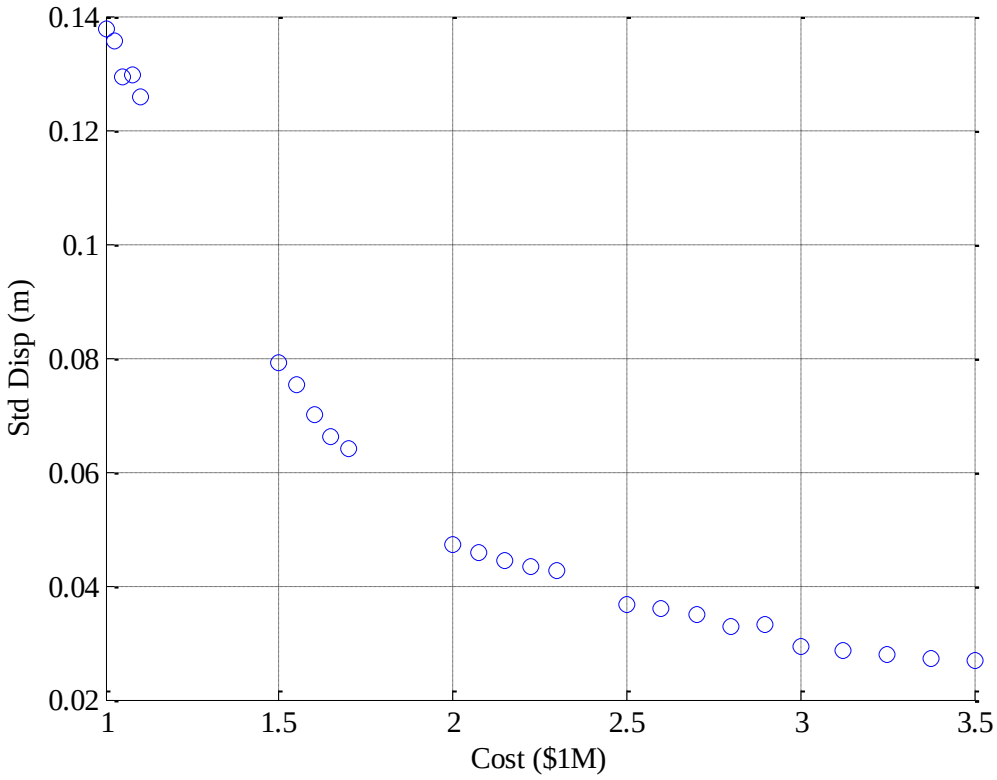

Figure 4.6 Pareto front for cost and standard deviation of max displacement relationship

From the Pareto front, four preferred designs are obtained using an overall measure ψ that accounts for three measures, cost measure c_r, safety measure S and robustness measure R. The measure ψ is defined in equation (4-14):

$$\psi = \sqrt{(\frac{c_r}{c_{max}})^2 + S^2 + R^2} \tag{4-14}$$

where c_{max} is the maximum of cost among all retrofit designs which is \$3.5M in our case. Each design has a corresponding ψ value. Four preferred designs are thus selected by picking lowest four ψ values among 25 retrofit designs. The details of the four preferred designs are shown in Table 4.3. The four preferred designs correspond to four strategies for each bridge. Together with the "do nothing" strategy, total five strategies are chosen to generate bridge damage scenarios used in the network level mode.

Table 4.3 Preferred design details

Design #	Cost c_r (\$1M)	Thickness w (mm)	Elasticity modulus E_s (GPa)
1	4.40	0.025	220
2	6.00	0.05	180
3	6.20	0.05	190
4	6.40	0.05	220

5.2 Sioux Falls Analysis

In this section, we demonstrate the application of the bi-level model through the use of the Sioux Falls network. Four bridges are located in the network, labeled as A, B, C and D.

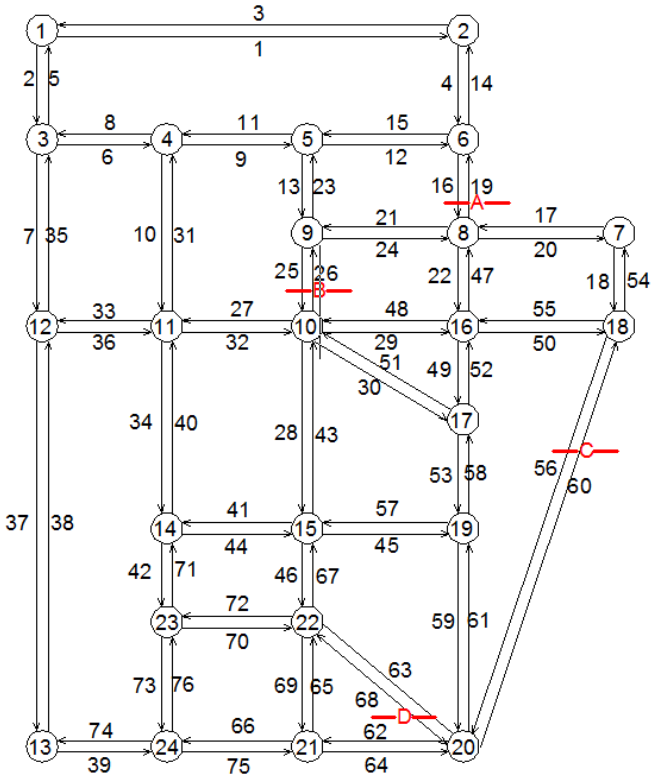

Figure 4.7 Sioux Falls Network

Generate bridge damage scenarios: The lower level problem yields four preferred designs from the whole design space where the four designs correspond to four strategies for each bridge at network level. Together with the "do nothing" strategy, the total five strategies are selected to generate bridge damage scenarios for network level model, where their maximum displacement values for different earthquakes are connected to traffic capacity. Table 4.4 shows the connection between different θ values for different maximum displacement range.

Table 4.4 Different θ values for different maximum displacement range

Max Disp. Range	θ Value	Max Disp. Range	θ Value
(0.5,1)	0.1	(0.02,0.05)	0.6
(0.3,0.5)	0.2	(0.01,0.02)	0.7
(0.2,0.3)	0.3	(0.005,0.01)	0.8
(0.1,0.2)	0.4	(0.002,0005)	0.9
(0.05,0.1)	0.5	(0,0.002)	1.0

We assume that the retrofit cost for a bridge is proportional to the size of the bridge. The sizes of bridge A and D are set to 1. Bridge B has size 2 and bridge C has size 3. The retrofit costs for different bridges under different retrofit strategies are provided in Table 4.5. Note that each bridge is represented by two directional links in this study.

Table 4.5 Retrofit cost ($1M) for all bridges

Bridges	Strategy				
	h0	h1	h2	h3	h4
link16	0	4.4	6	6.2	6.4
link19	0	4.4	6	6.2	6.4
link25	0	8.8	12	12.4	12.8
link26	0	8.8	12	12.4	12.8
link56	0	13.2	18	18.6	19.2
link60	0	13.2	18	18.6	19.2
link63	0	4.4	6	6.2	6.4
link68	0	4.4	6	6.2	6.4

The results of the baseline study is presented in Table 4.6, include the costs, strategies and solution performance under different budget levels ($20M, $30M, and $40M). The top section of the table reports different cost items. In particular, the objective value is the regret values, 1st stage cost is the retrofit cost, and mean 2nd stage cost is to take average of second stage system travel cost across different scenarios. The solution performances include the algorithm solution time, optimality gap, and iterations which are reported in the middle section of the table. Solution time is decomposed to the time of obtaining perfect information solutions and optimal regret solutions. The optimality gap shows the convergence of the algorithm. Lower optimality gap reflects higher quality of the solutions by the algorithm. The computing times and iterations indicate the efficiency of the algorithm. For the bottom section, explicitly details of optimal strategies applied to different bridges are reported.

Table 4.6 Baseline results under different budget levels

Items		Budget Levels		
		$20M	$30M	$40M
1st stage cost (10^6)		12.80	29.60	36.00
Mean 2nd stage cost (10^6)		329.21	310.16	301.71
CPU Time	Perfect Info.	54.38	93.72	119.57
(min)	Regret	15.57	25.92	46.62
Optimality Gap		0.00%	0.00%	0.00%
# of Iteration		4	7	13
Bridge A Strategy		h4	h2	h2
Bridge B Strategy		h0	h1	h2
Bridge C Strategy		h0	h0	h0
Bridge D Strategy		h0	h0	h0

We can see that the 1st stage cost increases due to increased budget level, which means that more costly strategies are selected. Also, as the increase of the total available budget, the mean 2nd stage cost decreases which indicate that the increased budget will help reduce the loss due to system travel delays. With increasing budget, the solution algorithm takes longer time and more number of iterations to find optimal solution, which is because the solution space is increased, and the problem becomes more difficult to solve when there are more feasible solutions. For all budget levels, the problems are solved with 0% optimality gap that indicates the problem is solved to optimality. Notice that the CPU times for obtaining perfect information solutions are much longer than the

time needed to solve regret problems. The reason for that is the perfect information solutions requires the NDP solved for each scenario separately which results in high CPU times. Strategies for bridge A and bridge B are changed when budgets are increasing while strategies for the other two bridges remain unchanged.

6. Conclusions

We developed a model framework that integrates seismic analysis into network level decision making process. The lower level framework captures the complex behavior of bridge structures when subject to earthquake excitation where a multi-objective optimization is conducted to find the Pareto front for the cost-safety-robustness relationship and further to produce a set of preferred retrofit designs. In particular, FE models with different designs are tested for different ground motions records. Safety and robustness measures are defined using the time histories results from FE models. At upper level, the set of preferred retrofit designs correspond to four strategies. Together with "do nothing" strategy, the five strategies are used to produce bridge damage scenarios to be used in the network level model. A two-stage minimax regret model is developed for transportation network resource allocation problem, which provides solutions with some level of robustness but less conservative compared to robust optimization method.

The model framework was demonstrated with a numerical example using 20 ground motion records and Sioux Falls network. Our method shows how to find a set of preferred

retrofit designs from the whole design space which may contains tens of even hundreds of possible designs. The results show that the increased budget will help reducing the loss due to system travel delays which requires more costly retrofit strategies.

There are several extensions to further enrich the context of this study. First, the study considers limited retrofit alternatives and bridge components. More enriching findings are possible by considering more type of retrofit alternatives and other bridge components. Second, future research can incorporate the uncertainty of retrofit outcomes. A specific retrofit design subject to the same disaster may have uncertain outcomes. By considering retrofit outcome uncertainties, new challenges are brought up to the network level modeling.

Chapter 5 Conclusions and Future Work

1. Conclusions

In Chapter 2, the research effort focuses on development of a novel formulation of retrofit resource allocation model at network level under earthquake uncertainty and a solution method to solve the model. Uncertainties in earthquakes are represented by discrete set of scenarios with made up values of bridge post-earthquake traffic capacities. The model captures the uncertainty through a stochastic modeling framework and is compromised by adding *CVaR* risk measure. It extends the existing literature in disaster management with multiple damage stages and multiple retrofit alternatives. The resulting model falls into a category of MINLP that is difficult to solve by using global solver. A decomposition method based on GBD is developed that can efficiently solve problem instance of large-scale benchmark network. The research in Chapter 2 can help decision makers allocate resources at network level with user-defined risk level.

In Chapter 3, network level model in Chapter 2 is couple with a lower level FE model. The FE model analyses bridge pier shearing performance under lateral loading and provides a Pareto frontier that reflects a nonlinear relationship of bridge resilient and cost. The Pareto frontier is then used at the upper level. The decisions made at upper level model using the nonlinear relationship assumption is compared with the decisions using simple linear resilient and cost assumption. It is the first attempt to integrate models from both levels which makes the decision making process at network level more realistic.

In Chapter 4, a hazard generation component is integrated into modeling framework and a formulation using minimax regret approach is developed to capture the earthquake uncertainty. In the literature, earthquake damages for bridges in a network are assumed to be given. It is not case in reality, where structures have complex behavior when subject to earthquake excitation. In Chapter 4, the integration of hazard component takes the structural seismic behavior into consideration. The methodology framework uses a set of earthquake scenarios represented by a set of ground motion records. By developing FE models with parameterized retrofit designs, the study captures the seismic response of bridges in the network. The seismic response of FE models are converted to earthquake scenarios with correlated damages of bridges in a transportation network. Another contribution is from the network modeling perspective. With the consideration of regret in each earthquake scenario, the proposed minimax regret approach can generate solutions that are robust but not over conservative. The proposed method avoids over conservatism by minimizing the worst-case regret.

The study proposed in this dissertation contributes to the fields of transportation infrastructure protection under natural hazard. The proposed work contributes the knowledge of modeling and solution algorithm of network level resource allocation model as well as robust design of infrastructure level model. Further, the proposed study integrates the two levels to obtain a sustainable infrastructure system, where they used to be considered and studied separately in the literature and in practice. Also, the proposed study will also aid in decision making in the resource allocation in a bridge network as well as retrofit decisions for individual infrastructure. Finally, this proposed study can be

used as a test bed for future bridge retrofit studies and it can provide baseline information for bridge retrofit schemes to be implemented in the real world.

2. Future Work

Sustainable and resilient infrastructure system development requires efforts from multiple disciplines and integration of these efforts. For bridge network protection, structural analyses are incorporated successfully into an optimization modeling framework to make better retrofit decisions at network and infrastructure level, which evokes more interdisciplinary researches that discuss below.

Develop sustainable energy infrastructure systems

With the rapid advancement of technology, the market penetration of alternative fuel vehicles (e.g. plug-in hybrid electric vehicles, battery electric vehicles) continues to grow. While the adoption of new technologies leads to a more efficient and innovative transportation system, the increase of alternative fuel vehicles also has imposed a high burden on local power grid. Questions such as how to optimize incentives to change travelers' behaviors towards energy conserving are also brought up. I plan to integrate travelers' behavior in sustainable energy infrastructure systems, focusing on the optimization of incentives to change travelers' behavior. The incentives include policy incentives as well as infrastructure investment based strategies, like the deployment of charging stations and electric highways for alternative fuel vehicles. Given the projected

electric vehicle market penetration and travel demands, I plan to combine the behavior incentives with infrastructure planning and maintenance optimization model to minimize overall cost function including energy consumption and greenhouse gas emission. This integrated research approach linking energy system modeling and travel behavior consideration will open up new collaborations with researchers across multiple disciplines and may attract external funding opportunities from federal agencies such as Department of Energy as well as private energy venture companies.

Improve the resiliency of transportation systems under uncertain disruptions

The aging of infrastructure increases the risk of infrastructure failure. Combined with hazardous weather situations and other disruptions, risky infrastructure would degrade traffic capacity, exacerbate congestion, and reduce accessibility to vital services. To mitigate the adverse impact of uncertain disruptions, I plan to integrate modeling of behavior change with resource allocation models. During disruption events, the travel demand may varies drastically because of potential trip cancellation due to high congestion levels and the alteration of trip purposes. Driver behavior may change as well during these events. The new models would try to capture these behavior changes through the exploration of new data collection technologies, mining of existing massive datasets, and testing of innovative data analysis methods.

Network design and applications in climate change adaptation

Climate change will lead to gradual environmental changes as well as more frequent and severe weather events, including hurricanes, heavy precipitation and extremely high

temperature. These changes have unclear impacts on demand variation and travel behavior, which makes the aforementioned problem more complex. In the past, I have worked on stochastic and robust network design problems. I plan to continue this research direction for transportation planning in pre-disaster mitigation and post-disaster recovery. My research will capture the effects of hurricane and heavy precipitation through collaboration with climatologist and developing stochastic programming models targeting hazard events to provide efficient retrofit plans.

Consider vehicle communication and automation technique on development of sustainable infrastructure system

Vehicle communication and automation system enables new capabilities for vehicles. Although developed to benefit individual vehicle, the new system may have potential influence on the traffic characteristic. The gradually introduction of vehicle communication technique will bring up new challenges in traffic management. Route guidance under extreme events is an interesting topic when we have partial information about network connectivity and road conditions. The coupling of vehicle communication systems and highway network systems under extreme events will be another research direction.

References

Ahmed, S. (2006). Convexity and decomposition of mean-risk stochastic programs. *Mathematical programming, 106*, 433-446.

Andersson, F., Mausser, H., Rosen, D., & Uryasev, S. (2001). Credit risk optimization with conditional value-at-risk criterion. *Mathematical programming, 89*, 273-291.

ANSYS."ANSYS Academic Research." (accessed).

ASCE."2013 Report Card for America's Infrastructure." infrastructurereportcard.org (accessed May 16, 2014).

Atamtürk, A., & Zhang, M. (2007). Two-stage robust network flow and design under demand uncertainty. *Operations Research, 55*, 662-673.

Augusti, G., Ciampoli, M., & Frangopol, D. M. (1998). Optimal planning of retrofitting interventions on bridges in a highway network. *Engineering Structures, 20*, 933-939.

Barbaroso, & gcaron, G. (2004). A two-stage stochastic programming framework for transportation planning in disaster response. *Journal of the Operational Research Society, 55*, 43-53.

Benders, J. F. (1962). Partitioning procedures for solving mixed-variables programming problems. *Numerische mathematik, 4*, 238-252.

Bertsimas, D., & Sim, M. (2003). Robust discrete optimization and network flows. *Mathematical Programming, 98*, 49-71.

Birge, J. R., & Louveaux, F. (2011). *Introduction to stochastic programming*: Springer.

Birge, J. R., & Louveaux, F. V. (1988). A multicut algorithm for two-stage stochastic linear programs. *European Journal of Operational Research, 34*, 384-392.

Bocchini, P., & Frangopol, D. M. (2011). Generalized bridge network performance analysis with correlation and time-variant reliability. *Structural Safety, 33*, 155-164.

Bonami, P., Biegler, L. T., Conn, A. R., Cornuéjols, G., Grossmann, I. E., Laird, C. D., Lee, J., Lodi, A., Margot, F., & Sawaya, N. (2008). An algorithmic framework for convex mixed integer nonlinear programs. *Discrete Optimization, 5*, 186-204.

Brown, N. J., Gearhart, J. L., Jones, D. A., Nozick, L. K., Romero, N., & Xu, N. (2013). Multi-objective optimization for bridge retrofit to address earthquake hazards. In *Winter Simulation Conference* (pp. 2475-2486).

Buckle, I., Friedland, I., Mander, J., Martin, G., Nutt, R., & Power, M. (2006). Seismic Retrofitting Manual for Highway Structures: Part 1 - Bridges. In.

Bureau of Public Roads. (1964). Manual traffic assignment. US Department of Commerce.

Burer, S., & Letchford, A. N. (2012). Non-convex mixed-integer nonlinear programming: A survey. *Surveys in Operations Research and Management Science, 17*, 97-106.

Carturan, F., Pellegrino, C., Rossi, R., Gastaldi, M., & Modena, C. (2013). An integrated procedure for management of bridge networks in seismic areas. *Bulletin of Earthquake Engineering, 11*, 543-559.

Chandrashekaran, S., & Banerjee, S. (2014). Optimal Retrofit Strategy for Disaster Resilience of Highway Bridges. In *10th US National Conference on Earthquake Engineering* (pp. 21-25).

Chang, L., Peng, F., Ouyang, Y., Elnashai, A., & Spencer, B. (2012). Bridge Seismic Retrofit Program Planning to Maximize Postearthquake Transportation Network Capacity. *Journal of Infrastructure Systems, 18*, 75-88.

Chang, L., Peng, F., Ouyang, Y., Elnashai, A. S., & Spencer Jr, B. F. (2012). Bridge seismic retrofit program planning to maximize postearthquake transportation network capacity. *Journal of Infrastructure Systems, 18*, 75-88.

Chen, B., Wang, J., Wang, L., He, Y., & Wang, Z. (2014). Robust optimization for transmission expansion planning: Minimax cost vs. minimax regret.

Drud, A. S. (1994). CONOPT—A Large-Scale GRG Code. *ORSA Journal on Computing, 6*, 207-216.

Duran, M. A., & Grossmann, I. E. (1986). An outer-approximation algorithm for a class of mixed-integer nonlinear programs. *Mathematical programming, 36*, 307-339.

Fábián, C. I. (2008). Handling CVaR objectives and constraints in two-stage stochastic models. *European Journal of Operational Research, 191*, 888-911.

Fan, Y., Liu, C., Lee, R., & Kiremidjian, A. S. (2010). Highway network retrofit under seismic hazard. *Journal of Infrastructure Systems, 16*, 181-187.

Federal Highway Administration."Highway Statistics Series: Highway Statistics 2010." http://www.fhwa.dot.gov/policyinformation/statistics/2010/vmt422.cfm (accessed Feb 23, 2015).

Federal Highway Administration."Highway Statistics Series: Motor Vehicles." http://www.fhwa.dot.gov/policyinformation/quickfinddata/qfvehicles.cfm (accessed Feb 23, 2015).

Furuta, H., Frangopol, D. M., & Nakatsu, K. (2011). Life-cycle cost of civil infrastructure with emphasis on balancing structural performance and seismic risk of road network. *Structure and Infrastructure Engineering, 7*, 65-74.

Geoffrion, A. M. (1972). Generalized benders decomposition. *Journal of optimization theory and applications, 10*, 237-260.

Golroo, A., Mohaymany, A. S., & Mesbah, M. (2010). Reliability based investment prioritization in transportation networks. In *Proceedings of the 89th annual meeting of the Transportation Research Board of the National Academies* (pp. 10-14).

Guo, Z. (2014). *Principles of reinforced concrete*: Butterworth-Heinemann.

Gupta, O. K., & Ravindran, A. (1985). Branch and bound experiments in convex nonlinear integer programming. *Management Science, 31*, 1533-1546.

Hong, L. J., & Liu, G. (2009). Simulating sensitivities of conditional value at risk. *Management Science, 55*, 281-293.

Huang, D., Zhu, S., Fabozzi, F. J., & Fukushima, M. (2010). Portfolio selection under distributional uncertainty: A relative robust CVaR approach. *European Journal of Operational Research, 203*, 185-194.

Huang, Y., Parmelee, S., & Pang, W. (2014). Optimal Retrofit Scheme for Highway Network under Seismic Hazards. *International Journal of Transportation Science and Technology, 3*, 109-128.

Inuiguchi, M., & Sakawa, M. (1995). Minimax regret solution to linear programming problems with an interval objective function. *European Journal of Operational Research, 86*, 526-536.

Kellerer, H., Pferschy, U., & Pisinger, D. (2004). *Knapsack problems*: Springer.

Kim, Y.-S., Spencer Jr, B. F., & Elnashai, A. S. (2008). Seismic loss assessment and mitigation for critical urban infrastructure systems. In: Newmark Structural Engineering Laboratory. University of Illinois at Urbana-Champaign.

Kouvelis, P., & Yu, G. (1997). *Robust discrete optimization and its applications* (Vol. 14): Springer.

Kouvelis, P., & Yu, G. (2013). *Robust discrete optimization and its applications* (Vol. 14): Springer Science & Business Media.

Kwon, C. (2011). Conditional value-at-risk model for hazardous materials transportation. In *Simulation Conference (WSC), Proceedings of the 2011 Winter* (pp. 1703-1709): IEEE.

Lampropoulos, A., & Dritsos, S. E. (2011). Modeling of RC columns strengthened with RC jackets. *Earthquake Engineering & Structural Dynamics, 40*, 1689-1705.

Laporte, G., & Louveaux, F. V. (1993). The integer L-shaped method for stochastic integer programs with complete recourse. *Operations research letters, 13*, 133-142.

LeBlanc, L. J. (1975). An algorithm for the discrete network design problem. *Transportation science, 9*, 183-199.

LeBlanc, L. J., Morlok, E. K., & Pierskalla, W. P. (1975). An efficient approach to solving the road network equilibrium traffic assignment problem. *Transportation Research, 9*, 309-318.

Lee, Y.-J., Song, J., Gardoni, P., & Lim, H.-W. (2011). Post-hazard flow capacity of bridge transportation network considering structural deterioration of bridges. *Structure and Infrastructure Engineering, 7*, 509-521.

Liu, C., Fan, Y., & Ordóñez, F. (2009). A two-stage stochastic programming model for transportation network protection. *Computers & Operations Research, 36*, 1582-1590.

Liu, M., & Frangopol, D. M. (2006). Optimizing bridge network maintenance management under uncertainty with conflicting criteria: Life-cycle maintenance, failure, and user costs. *Journal of structural engineering, 132*, 1835-1845.

Lou, Y., Yin, Y., & Lawphongpanich, S. (2009). Robust approach to discrete network designs with demand uncertainty. *Transportation Research Record*, 86-94.

Lu, J., Huang, Y., & Gupte, A. (2015). A Risk-averse Two-stage Stochastic Programming Model For Transportation Network Protection Problems. In *Transportation Research Board 94th Annual Meeting*.

Luathep, P., Sumalee, A., Lam, W. H., Li, Z.-C., & Lo, H. K. (2011). Global optimization method for mixed transportation network design problem: a mixed-integer linear programming approach. *Transportation Research Part B: Methodological, 45*, 808-827.

Mackie, K., & Stojadinovic, B. (2004). Residual displacement and post-earthquake capacity of highway bridges. In *Proceedings of the Thirteenth World Conference on Earthquake Engineering*.

Magnanti, T. L., & Wong, R. T. (1984). Network design and transportation planning: Models and algorithms. *Transportation science, 18*, 1-55.

McNally, M. G. (2008). The four step model. *Center for Activity Systems Analysis*.

Mohaymany, A. S., & Pirnazar, N. (2007). Critical routes determination for emergency transportation network aftermath earthquake. In *Industrial Engineering and Engineering Management, 2007 IEEE International Conference on* (pp. 817-821): IEEE.

Nagurney, A. (2006). *Supply Chain Network Economics: Dynamics of Prices, Flows, and Profits*. Cheltenham, England: Edward Elgar Publishing.

Nagurney, A. (2007). Mathematical Models of Transportation and Networks. In W.-B. Zhang (Ed.), *Mathematical Models in Economics*.

NISEE."Suites of Earthquake Ground Motions for Analysis of Steel Moment Frame Structures." http://nisee.berkeley.edu/data/strong_motion/sacsteel/ground_motions.html (accessed August 30, 2015).

Nishida, H., & Unjoh, S. (2004). Dynamic response characteristic of reinforced concrete column subjected to bilateral earthquake ground motions. In *Proceedings 13th World Conference on Earthquake Engineering, Vancouver, Canada, Paper* (Vol. 576).

Noyan, N. (2012). Risk-averse two-stage stochastic programming with an application to disaster management. *Computers & Operations Research, 39*, 541-559.

Patriksson, M. (1994). *The traffic assignment problem: models and methods*. The Netherlands: VSP.

Peeta, S., Salman, F. S., Gunnec, D., & Viswanath, K. (2010). Pre-disaster investment decisions for strengthening a highway network. *Computers & Operations Research, 37*, 1708-1719.

Peeta, S., & Ziliaskopoulos, A. (2001). Foundations of Dynamic Traffic Assignment: The Past, the Present and the Future. *Networks and Spatial Economics, 1*, 233-265.

Priestley, M. N., Verma, R., & Xiao, Y. (1994). Seismic shear strength of reinforced concrete columns. *Journal of structural engineering, 120*, 2310-2329.

Quesada, I., & Grossmann, I. E. (1992). An LP/NLP based branch and bound algorithm for convex MINLP optimization problems. *Computers & chemical engineering, 16*, 937-947.

Rockafellar, R. T., & Uryasev, S. (2000). Optimization of conditional value-at-risk. *Journal of risk, 2*, 21-42.

Rockafellar, R. T., & Uryasev, S. (2002). Conditional value-at-risk for general loss distributions. *Journal of banking & finance, 26*, 1443-1471.

Rokneddin, K., Ghosh, J., Dueñas-Osorio, L., & Padgett, J. E. (2013). Bridge retrofit prioritisation for ageing transportation networks subject to seismic hazards. *Structure and Infrastructure Engineering, 9*, 1050-1066.

Rokneddin, K., Ghosh, J., Padgett, J. E., & Osorio, L. D. (2011). The Effects of Deteriorating Bridges on Bridges on the Bridge Network Connectivity. In *Structures Congress 2011* (pp. 2993-3007): ASCE.

Ruiwei, J., Jianhui, W., Muhong, Z., & Yongpei, G. (2013). Two-Stage Minimax Regret Robust Unit Commitment. *IEEE Transactions on Power Systems, 28*, 2271-2282.

Schultz, R., & Tiedemann, S. (2006). Conditional value-at-risk in stochastic programs with mixed-integer recourse. *Mathematical programming, 105*, 365-386.

Shao, L., Qin, X., & Xu, Y. (2011). A conditional value-at-risk based inexact water allocation model. *Water resources management, 25*, 2125-2145.

Sheffi, Y. (1985). *Urban Transportation Networks: Equilibrium Analysis With Mathematical Programming Methods*. Englewood Cliffs, NJ: Prentice Hall.

Shinozuka, M., Murachi, Y., Dong, X., Zhou, Y., & Orlikowski, M. J. (2003). Effect of seismic retrofit of bridges on transportation networks. *Earthquake Engineering and Engineering Vibration, 2*, 169-179.

Smith, E. M., & Pantelides, C. C. (1999). A symbolic reformulation/spatial branch-and-bound algorithm for the global optimisation of nonconvex MINLPs. *Computers & chemical engineering, 23*, 457-478.

Sohn, J., Kim, T. J., Hewings, G. J., Lee, J. S., & Jang, S.-G. (2003). Retrofit priority of transport network links under an earthquake. *Journal of Urban Planning and Development, 129*, 195-210.

Sun, H., Gao, Z., & Long, J. (2011). The robust model of continuous transportation network design problem with demand uncertainty. *Journal of Transportation Systems Engineering and Information Technology, 11*, 70-76.

Sun, Z., Si, B., Wang, D., & Guo, X. (2008). Experimental research and finite element analysis of bridge piers failed in flexure-shear modes. *Earthquake Engineering and Engineering Vibration, 7*, 403-414.

Toso, E. A. V., & Alem, D. (2014). Effective location models for sorting recyclables in public management. *European Journal of Operational Research, 234*, 839-860.

Uryasev, S. (2000). Conditional value-at-risk: Optimization algorithms and applications. In *Computational Intelligence for Financial Engineering, 2000.(CIFEr) Proceedings of the IEEE/IAFE/INFORMS 2000 Conference on* (pp. 49-57): IEEE.

Viswanath, K., & Peeta, S. (2003). Multicommodity maximal covering network design problem for planning critical routes for earthquake response. *Transportation Research Record: Journal of the Transportation Research Board, 1857*, 1-10.

Wang, Q., Fang, H., & Zou, X.-K. (2010). Application of Micro-GA for optimal cost base isolation design of bridges subject to transient earthquake loads. *Structural and Multidisciplinary Optimization, 41*, 765-777.

Westerlund, T., & Pettersson, F. (1995). An extended cutting plane method for solving convex MINLP problems. *Computers & chemical engineering, 19*, 131-136.

Xu, S. Y., & Zhang, J. (2011). Hysteretic shear–flexure interaction model of reinforced concrete columns for seismic response assessment of bridges. *Earthquake Engineering & Structural Dynamics, 40*, 315-337.

Yafeng, Y., Madanat, S. M., & Xiao-Yun, L. (2009). Robust improvement schemes for road networks under demand uncertainty. *European Journal of Operational Research, 198*, 470-479.

Yang, H., & H. Bell, M. G. (1998). Models and algorithms for road network design: a review and some new developments. *Transport Reviews, 18*, 257-278.

Yau, S., Kwon, R. H., Scott Rogers, J., & Wu, D. (2011). Financial and operational decisions in the electricity sector: contract portfolio optimization with the conditional value-at-risk criterion. *International Journal of Production Economics, 134*, 67-77.

Zhang, J., Xu, S. Y., & Tang, Y. (2011). Inelastic displacement demand of bridge columns considering shear–flexure interaction. *Earthquake Engineering & Structural Dynamics, 40*, 731-748.

Zhang, M. (2011). Two-stage minimax regret robust uncapacitated lot-sizing problems with demand uncertainty. *Operations research letters, 39*, 342-345.

Zhou, Y., Banerjee, S., & Shinozuka, M. (2010). Socio-economic effect of seismic retrofit of bridges for highway transportation networks: a pilot study. *Structure and Infrastructure Engineering, 6*, 145-157.

Zhou, Y., Murachi, Y., Kim, S.-H., & Shinozuka, M. (2004). Seismic risk assessment of retrofitted transportation systems. In *Proceedings of the 13 th World Conference on Earthquake Engineering*.